*Research Article*

INTERNATIONAL JOURNAL OF ADVANCED ROBOTIC SYSTEMS

*International Journal of Advanced Robotic Systems*
March-April 2017: 1–17

DOI: 10.1177/1729881416687504
journals.sagepub.com/home/arx
SAGE

# Efficient adaptive constrained control with time-varying predefined performance for a hypersonic flight vehicle

**Caisheng Wei[1], Jianjun Luo[1], Honghua Dai[1], Jianping Yuan[1] and Jianfeng Xie[2]**

## Abstract

A novel low-complexity adaptive control method, capable of guaranteeing the transient and steady-state tracking performance in the presence of unknown nonlinearities and actuator saturation, is investigated for the longitudinal dynamics of a generic hypersonic flight vehicle. In order to attenuate the negative effects of classical predefined performance function for unknown initial tracking errors, a modified predefined performance function with time-varying design parameters is presented. Under the newly developed predefined performance function, two novel adaptive controllers with low-complexity computation are proposed for velocity and altitude subsystems of the hypersonic flight vehicle, respectively. Wherein, different from neural network-based approximation, a least square support vector machine with only two design parameters is utilized to approximate the unknown hypersonic dynamics. And the relevant ideal weights are obtained by solving a linear system without resorting to specialized optimization algorithms. Based on the approximation by least square support vector machine, only two adaptive scalars are required to be updated online in the parameter projection method. Besides, a new finite-time-convergent differentiator, with a quite simple structure, is proposed to estimate the unknown generated state variables in the newly established normal output-feedback formulation of altitude subsystem. Moreover, it is also employed to obtain accurate estimations for the derivatives of virtual controllers in a recursive design. This avoids the inherent drawback of backstepping — "explosion of terms" and makes the proposed control method achievable for the hypersonic flight vehicle. Further, the compensation design is employed when the saturations of the actuator occur. Finally, the numerical simulations validate the efficiency of the proposed finite-time-convergent differentiator and control method.

## Keywords

Hypersonic flight vehicle, least square support vector machine, backstepping, predefined performance, finite-time-convergent differentiator, actuator saturation

Date received: 10 June 2016; accepted: 13 December 2016

Topic: Special Issue – Control of Hypersonic Flight Vehicles
Topic Editor: Danwei Wang

## Introduction

Recently hypersonic flight vehicles (HFVs) have drawn growing attention since they are promising to provide a reliable and cost-efficient way to explore space for critical military and commercial applications.[1] However, owing to the peculiarities of vehicle dynamics such as high nonlinearity, parametric uncertainties and complex coupling, the resulting control system design is a very challenging task and remains open.[2]

[1] National Key Laboratory of Aerospace Flight Dynamics, Northwestern Polytechnical University, Xi'an, China
[2] Beijing Aerospace Control Center, Beijing, China

**Corresponding author:**
Jianjun Luo, National Key Laboratory of Aerospace Flight Dynamics, Northwestern Polytechnical University, Xi'an 710072, China.
Email: jjluo@nwpu.edu.cn

Currently only the longitudinal models of HFVs are broadly studied considering the tedious complexity of their dynamics.[3–7] Benefiting from the cascade structure of HFV dynamics, a strict-feedback form of the altitude subsystem was obtained and then a backstepping technique was utilized to devise the state-feedback controller in the work by Wu and Meng and Xu et al.[8–10] Although the backstepping technique has been evolved as an efficient control method for HFVs, tedious and complex analysis is required for virtual controllers and their repeated derivatives. This is the inherent drawback of backstepping, also referred to as "explosion of terms".[11] In order to overcome this demerit, dynamic surface control was employed to facilitate the controller design by letting the virtual command pass through a first-order filter.[11–14] In order to further eliminate the complexity of the immediate controllers in the recursive design, a hyperbolic-sine-function-based tracking differentiator was constructed to obtain good estimations for the derivatives of virtual controllers involved in the control system design of an air-breathing hypersonic vehicle (AHV) in the work by Bu et al.[15] However, some issues are still open for differentiators such as a good dynamic response and high estimation accuracy.

Considering the unknown nonlinearities existing in HFVs, the neural network (NN) is widely used as an efficient tool for nonlinear approximation.[9–13,16] But reducing the complexity of NN-based approximators is necessary and is needed for HFVs because of their fast dynamic characteristics. Meanwhile, due to the learning mechanism of the NN, its training process is based on empirical risk minimization which means the learning of NN seeks the smallest learning errors. This tends to induce under-fitting and over-fitting phenomena. To obtain a simple approximator for unknown dynamics existing in a HFV, some new techniques are needed. Thanks to Vapnik's support vector machine (SVM) theory,[17] good generalization ability is observed and it can solve small sample problems based on the principles of structural risk minimization. Besides, a SVM can overcome the intrinsic demerits including the under-fitting and over-fitting phenomena. However, the required constrained optimization programming leads to a higher computational burden, which is the major drawback of a SVM. In order to surmount this drawback, least square SVM (LS-SVM), a computationally attractive machine learning technique, was proposed by Suykens and Vandewalle, which works with equality instead of inequality constraints in the optimization.[18] This greatly simplifies the optimization problem such that the relevant optimal solution is characterized by a linear system according to the first-order Karush–Kuhn–Tucker (KKT) optimality conditions. Through solving the linear system, the optimal solution can be obtained efficiently. Comparing with the NN, the optimal solution is global without any help from other optimization techniques such as the quadratic programming method and the dynamic programming method. Thus, the LS-SVM was widely utilized in the approximation of unknown dynamics.[19–21] Owing to the attractively computational advantage, the LS-SVM is more advantageous in handling the approximation of unknown hypersonic dynamics.

Another crucial issue associated with the adaptive control of a HFV is the transient (such as overshoot, undershoot, and convergence rate) and steady-state tracking performance. In practice, ensuring a high fidelity transient and steady-state tracking performance is very challenging. Recently, Bechlioulis and Rovithakis developed a new control design and synthesis methodology,[22, 23] in which the transient and steady-state performance is quantitatively characterized and limited by an appropriate predefined (or prescribed) performance function (labeled as classical predefined performance function [CPPF]). This control method was further explored for nonlinear systems subject to input nonlinearity[24–26]. However, in particular, there exists very little work which aims to quantitatively and accurately compute the transient tracking performance of a HFV. Yang and Chen applied a CPPF to realize the predefined performance attitude tracking control of near-space vehicles.[27] Bu et al. utilized a CPPF to construct two guaranteed transient performance-based adaptive neural controllers for velocity and altitude subsystems of AHVs, respectively.[28] However, some limitations are encountered in the CPPF. The first one is that the initial tracking errors of the controlled system must be remained strictly within a predefined region. In general, however, the initial tracking errors are hard to obtain in the presence of the uncertainties and external disturbances, especially for a HFV with strong uncertainties. Thus, it is hard to guarantee that the initial tracking errors are enveloped within the predefined region formed by the designed CPPF. Besides, the fixed parameters in a CPPF result in a much larger conservative estimation of the tracking performance bound. Therefore, a novel predefined performance function is required to avoid these limitations.

In this article, we mainly focus on the adaptive tracking controller with a low complexity design for a HFV subject to unknown nonlinearities and actuator saturation. In order to lower the conservativeness of the CPPF, eliminate the growing complexity of backstepping, tackle the state observation, and reduce computational complexity of the NN in approximating unknown hypersonic dynamics, we propose a novel adaptive control method with only two adaptive scalars that need to be updated online. Simultaneously, there are only two design parameters contained in the LS-SVM-based approximators. Compared with the previous studies, the adaptive mechanism and nonlinear approximation with a much simpler structure are achievable for HFV. Thus, the computational burden is lighter. The contribution of our work is threefold.

1. A time-varying predefined performance function (TPPF) is first proposed. Compared with the CPPF, it can address the problem of unknown initial tracking errors and lower the conservativeness of the CPPF over the estimation of the performance bound. The design of the controllers is carried out under the proposed TPPF throughout the entire article.

2. A novel finite-time-convergent differentiator (FTCD) with a simple structure is proposed. The newly established FTCD is applied to obtain good estimations of the derivatives of the virtual controllers rapidly, with high accuracy. This conquers the inherent drawback of backstepping – "explosion of terms". Besides, the newly defined state variables in the normal output-feedback system are observed precisely by the proposed FTCD.
3. Two LS-SVM based approximators are constructed to approximate the unknown hypersonic dynamics. No specialized optimization algorithms are required because the relevant ideal weights are obtained by solving a linear system. This significantly decreases the computational complexity of nonlinear approximation. Besides, by estimating the norm of ideal weights rather than their elements, only two adaptive parameters are updated online in the parameter projection method which simplifies the adaptation laws.

## Problem statement and preliminaries

### Model description

The longitudinal dynamics of a generic HFV developed by Parker et al. is considered in this article.[29] This model involves five rigid-body variables $X = [V, h, \alpha, \gamma, q]$ and two saturated system inputs $U = [\delta_e, \Phi]^{\mathrm{T}}$. The equations of motion of this model are expressed by

$$\begin{cases} \dot{V} = \dfrac{T\cos\alpha - D}{m} - g\sin\gamma \\ \dot{h} = V\sin\gamma \\ \dot{\gamma} = \dfrac{L + T\sin\alpha}{mV} - \dfrac{g\cos\gamma}{V} \\ \dot{\alpha} = q - \dot{\gamma} \\ \dot{q} = \dfrac{M_{yy}}{I_{yy}} \end{cases} \tag{1}$$

with $T \approx T_\Phi(\alpha)\Phi + T_0(\alpha) = (\beta_1\Phi + \beta_2)\alpha^3 + (\beta_3\Phi + \beta_4)\alpha^2 + (\beta_5\Phi + \beta_6)\alpha + (\beta_7\Phi + \beta_8)$, $L \approx \bar{q}S_a(C_L^\alpha\alpha + C_L^0)$, $D \approx \bar{q}S_a(C_D^{\alpha^2}\alpha^2 + C_D^\alpha\alpha + C_D^0)$, $M_{yy} \approx z_T T + \bar{q}S_a\bar{c}(C_M^{\alpha^2}\alpha^2 + C_M^\alpha\alpha + C_M^0) + \bar{q}S_a\bar{c}C_M^{\delta_e}\delta_e$, $\bar{q} = \frac{1}{2}\rho V^2$, $\rho = \rho_0\,\mathrm{e}^{-(h-h_0)/h_s}$.

Assume that the five state variables are available for measurement. The system inputs $\delta_e, \Phi$ are subject to the following asymmetric or symmetric saturations

$$\delta_e = \mathrm{sat}(v_{\delta_e}) = \begin{cases} u_{M1}^+, & \text{if } v_{\delta_e} \geq u_{M1}^+ \\ v_{\delta_e}, & \text{otherwise} \\ u_{M1}^-, & \text{if } v_{\delta_e} \leq u_{M1}^- \end{cases},$$
$$\Phi = \mathrm{sat}(v_\Phi) = \begin{cases} u_{M2}^+, & \text{if } v_\Phi \geq u_{M2}^+ \\ v_\Phi, & \text{otherwise} \\ u_{M2}^-, & \text{if } v_\Phi \leq u_{M2}^- \end{cases} \tag{2}$$

where $|u_{Mi}^+|$, $|u_{Mi}^-|(i = 1, 2)$ are the bounds of the system inputs.

Based on functional decomposition, the dynamics in equation (1) can be divided into a velocity subsystem and a altitude subsystem. For the velocity subsystem, for brevity, it can be written as

$$\begin{cases} \dot{V} = f_V + \Phi \\ y_V = V \end{cases} \tag{3}$$

where $y_V$ is the output of the velocity subsystem. $f_V = (T\cos\alpha - D)/m - g\sin\gamma - \Phi$ is assumed to be completely unknown and needs to be estimated by a LS-SVM-based approximator.

As for the altitude subsystem, define the altitude tracking error as $\tilde{h} = h - h_r$. From equation (1), one can find that when $\gamma$ tracks the given command $\gamma_d$, then $\tilde{h}$ can be regulated to zero stably. Therefore, the task of altitude subsystem is to design an approximate controller $v_\Phi$ to track the command $\gamma_d$ whose detailed form is given later. First, define $x_1 = \gamma$, $x_2 = \alpha + \gamma$, $x_3 = q$, then we can obtain

$$\begin{cases} \dot{x}_1 = f_{h1}(\bar{x}_2) + x_2 \\ \dot{x}_2 = x_3 \\ \dot{x}_3 = f_{h2}(\bar{x}_3) + \delta_e \\ y_h = x_1 \end{cases} \tag{4}$$

where $y_h$ is the output of the altitude system, $\bar{x}_i = [x_1, \ldots, x_i]^{\mathrm{T}}(i = 2, 3)$, $f_{h1}(\bar{x}_2) = (L + T\sin\alpha)/(mV) - g\cos\gamma/V - x_2$, $f_{h2}(\bar{x}_3) = M_{yy}/I_{yy} - \delta_e$. Inspired by Xu et al.,[30] in order to reduce the number of LS-SVM-based approximators for unknown terms $f_{h1}, f_{h2}$, an output-feedback system in a norm form is developed as follows instead of the state-feedback one in equation (4), that is

$$\begin{cases} \dot{z}_1 = z_2 \\ \dot{z}_2 = z_3 \\ \dot{z}_3 = a(\bar{x}_3) + \delta_e \end{cases} \tag{5}$$

with $a(\bar{x}_3) = \frac{\partial b(\bar{x}_3)}{\partial x_1}(f_{h1}(\bar{x}_2) + x_2) + \frac{\partial b(\bar{x}_3)}{\partial x_2}x_3 + \frac{\partial b(\bar{x}_3)}{\partial x_3}(f_{h2}(\bar{x}_3) + \delta_e) + f_{h2}(\bar{x}_3)$, $b(\bar{x}_3) = \frac{\partial f_{h1}(\bar{x}_2)}{\partial x_1}(f_{h1}(\bar{x}_2) + x_2) + \frac{\partial f_{h1}(\bar{x}_2)}{\partial x_2}x_3$. ($z_1 = y_h$, $z_2 = \dot{y}_h$, $z_3 = \ddot{y}_h$).

Seeing from equation (5), only one LS-SVM-based approximator needs to design for unknown term $a(\bar{x}_3)$ rather than two ones for the unknown $f_{h1}, f_{h2}$. However, the newly defined state variables $z_2, z_3$ are not available for measurement except when $z_1 = \gamma$. Thus, a FTCD is devised to observe them.

### Control objective

The objective pursued in this work is to shrink the tracking errors $\tilde{V} = V - V_r$ and $\tilde{h}$ stably with a time-varying bounded transient and steady-state performance in spite of the coexistence of unknown nonlinearities and input saturation. In detail, the objective is twofold:

(a) design a low-complexity LS-SVM-based adaptive controller $v_\Phi$ to steer the velocity $V$ to track its command $V_r$ stably in the presence of unknown $f_V$ and saturation of fuel equivalence ratio with guaranteed prescribed performance;
(b) design a LS-SVM-based adaptive controller $v_{\delta_e}$ with low complexity to steer $\gamma$ to track its command $\gamma_d$ stably subject to unknown $a(\bar{x}_3)$ and saturation of the elevator deflection with guaranteed prescribed performance.

### Time-varying predefined performance function

To quantitatively study the transient and steady-state performance of the tracking error $e(t)$, a smooth, strictly positive decaying function $\mu(t):\mathbb{R}_{\geq 0}\to\mathbb{R}^+$ with $\lim_{t\to\infty}\mu(t)=\mu_\infty>0$ is chosen as the predefined function, just like a CPPF. It is sufficient to achieve the transient and steady-state performance if the following condition holds

$$-\delta_1(t)\mu(t)<e(t)<\delta_2(t)\mu(t) \tag{6}$$

where $\delta_1(t)$, $\delta_2(t)$ are the positive design time-varying parameters and $\mu(t)$, $\delta_1(t)$, $\delta_2(t)$ in this work are chosen as

$$\begin{cases}\mu(t)=(\mu_0-\mu_\infty)e^{-\kappa_0 t}+\mu_\infty\\ \delta_1(t)=(\delta_{10}-\delta_{1\infty})e^{-\kappa_1 t}+\delta_{1\infty}\\ \delta_2(t)=(\delta_{20}-\delta_{2\infty})e^{-\kappa_2 t}+\delta_{2\infty}\end{cases} \tag{7}$$

where $\mu_0$, $\mu_\infty$, $\delta_{10},\delta_{1\infty}$, $\delta_{20},\delta_{2\infty}$ $\kappa_0$, $\kappa_1$, $\kappa_2$ are positive design constants.

**Remark 1.** Different from a CPPF with fixed $\delta_1,\delta_2$ in previously reported works,[22–28] in this work, $\delta_1(t),\delta_2(t)$ are time-varying rather than time-invariant. This implies that the ultimate tracking accuracies defined by the TPPF and CPPF are limited in the following bounds, respectively

$$-\delta_{1\infty}\mu_\infty<\lim_{t\to\infty}e(t)<\delta_{2\infty}\mu_\infty \tag{8a}$$

$$-\mu_\infty<\lim_{t\to\infty}e(t)<\mu_\infty \tag{8b}$$

Comparing equations (8a) and (8b), we can find the bound of ultimate tracking accuracy defined by the TPPF has lower conservativeness due to the additional parameters $\delta_{1\infty}$, $\delta_{2\infty}$. Namely, if $\delta_{1\infty},\delta_{2\infty}\leq 1$, a higher tracking accuracy can be achieved without considering the limitations of a control input under a TPPF. Under the proposed TPPF, define the tracking error $e(t)\triangleq\mu(t)P(s(t))$, where $s$ is the transformed error. Choose the function $P(s)$ as

$$P(s(t))=\frac{\delta_2(t)e^s-\delta_1(t)e^{-s}}{e^s+e^{-s}} \tag{9}$$

It is easy to find that $\lim_{s\to\infty}P(s)=\delta_2(t)$, $\lim_{s\to-\infty}P(s)=-\delta_1(t)$. Whilst, the chosen function $P(s)$ is strictly monotonic increasing and satisfies $P(0)\neq 0$. Thus, the transformed error $s(t)$ can be obtained as

$$s(t)=\frac{1}{2}\ln\left(\frac{\delta_1+\Lambda}{\delta_2-\Lambda}\right),\ \Lambda\triangleq\frac{e(t)}{\mu(t)} \tag{10}$$

Take its derivative as

$$\begin{aligned}\dot{s}(t)&=\frac{\partial s(t)}{\partial\Lambda(t)}\cdot\frac{d\Lambda(t)}{dt}+\frac{\partial s(t)}{\partial\delta_1(t)}\cdot\frac{d\delta_1(t)}{dt}+\frac{\partial s(t)}{\partial\delta_2(t)}\cdot\frac{d\delta_2(t)}{dt}\\&=\varepsilon[\dot{e}_1(t)-\Lambda\dot{\mu}(t)+\delta_c/\varepsilon]\end{aligned} \tag{11}$$

with $\varepsilon=\frac{1}{2\mu(t)}\cdot\left(\frac{1}{\delta_1+\Lambda(t)}+\frac{1}{\delta_2-\Lambda(t)}\right)$, $\delta_c=\frac{1}{2}\left(\frac{1}{\delta_1+\Lambda(t)}\dot{\delta}_1-\frac{1}{\delta_2-\Lambda(t)}\dot{\delta}_2\right)$.

Equation (11) is applied to construct the transformed tracking errors of $\tilde{V}$, $\tilde{h}$ under TPPF in the following work, respectively.

### LS-SVM-based approximation

To approximate the unknown nonlinearities, the LS-SVM is adopted due to its powerful generalization superiority and fast computational efficiency. The process of approximating the unknown nonlinear function with LS-SVM is as follows.[18]

First, choose the training sample set $SE=\{\pi_i,Y_i|,\ \pi_i\in\mathbb{R}^n,\ Y_i\in\mathbb{R},\ i=1,2,\ldots,N\}$ with $\pi_i$, $Y_i$, and $N$ being, respectively, the input vectors, output, and total number of the training samples of the LS-SVM-based approximator. The relevant estimation problem is expressed by

$$Y(\pi)=W^{\mathrm{T}}K(\pi)+p \tag{12}$$

where the superscript T denotes the transpose of a vector or matrix. $K(\cdot):\mathbb{R}^n\to\mathbb{R}^{n_h}$ is a known function mapping the input vector into a feature space of high dimension. $W$ and $p$ represent the weight and bias, respectively. Then the corresponding optimization problem of equation (12) to determine the ideal weight is expressed by

$$\begin{aligned}&V_{(W,p,\varpi)}=\frac{1}{2}\|W\|^2+\frac{c_0}{2}\sum_{i=1}^{N}\varpi_i^2\\&\text{s.t. } Y_i(\pi_i)=W^{\mathrm{T}}K(\pi_i)+p+\varpi_i\end{aligned} \tag{13}$$

where $c_0$ and $\varpi_i$ denote the positive regulation parameter and $i$th approximation error, respectively. The Lagrange function of equation (13) is

$$\begin{aligned}La=&\frac{1}{2}\|W\|^2+\frac{c_0}{2}\sum_{i=1}^{N}\varpi_i^2\\&-\sum_{i=1}^{N}\bar{\theta}_i\left(W^{\mathrm{T}}K(\pi_i)+p+\varpi_i-Y_i(\pi_i)\right)\end{aligned} \tag{14}$$

where $\bar{\theta}_i$ are the Lagrange multipliers. The first-order KKT optimality conditions of equation (14) are obtained as

$$\begin{cases} \dfrac{\partial La}{\partial W} = 0 \Rightarrow W = \sum_{i=1}^{N} \bar{\theta}_i K(\pi_i) \\ \dfrac{\partial La}{\partial p} = 0 \Rightarrow \sum_{i=1}^{N} \bar{\theta}_i = 0 \\ \dfrac{\partial La}{\partial \varpi_i} = 0 \Rightarrow c_0 \varpi_i - \bar{\theta}_i = 0 \\ \dfrac{\partial La}{\partial \bar{\theta}_i} = 0 \Rightarrow W^{\mathrm{T}} K(\pi_i) + p + \varpi_i - Y_i(\pi_i) = 0 \end{cases} \tag{15}$$

Further, equation (15) is equivalent to the following linear system

$$\begin{bmatrix} 0 & \vec{1}^{\mathrm{T}} \\ \vec{1} & \Omega + c_0^{-1} I \end{bmatrix} \begin{bmatrix} p \\ \bar{\theta} \end{bmatrix} = \begin{bmatrix} 0 \\ \Theta \end{bmatrix} \tag{16}$$

where $\vec{1} = [1, \ldots, 1]^{\mathrm{T}} \in \mathbb{R}^N$. $\Omega_{ij} = \varphi(\pi_i, \pi_j) = K^{\mathrm{T}}(\pi_i) \cdot K(\pi_j)\ (i,j = 1, 2, \ldots, N)$ is the kernel function. $\Theta \triangleq [Y_1, Y_2, \ldots, Y_N]^{\mathrm{T}}$ and $\bar{\theta} \triangleq [\bar{\theta}_1, \bar{\theta}_2, \ldots, \bar{\theta}_N]^{\mathrm{T}}$. In our work, the Gaussian kernel function $\varphi(\pi, \pi_i) = e^{[-(\pi-\pi_i)^{\mathrm{T}}(\pi-\pi_i)^{\mathrm{T}}/(2\zeta^2)]}$ is chosen, where $\zeta^2$ is the square bandwidth of the receptive field. Define $A \triangleq \Omega + c_0^{-1} I$ and A as invertible considering $\Omega_{ij} \geq 0, c > 0$. Then we can obtain

$$\begin{cases} p = \dfrac{\vec{1}^{\mathrm{T}} A^{-1} \Theta}{\vec{1}^{\mathrm{T}} A^{-1} \vec{1}} \\ \bar{\theta} = A^{-1}(\Theta - p\vec{1}) \end{cases} \tag{17}$$

Then, the approximation function in equation (12) is equal to

$$Y(\pi) = \sum_{i=1}^{N} \bar{\theta}_i \varphi(\pi, \pi_i) + p \tag{18}$$

For brevity, equation (18) is defined as

$$\begin{cases} Y(\pi) \triangleq \theta \varphi(\pi) \\ \theta \triangleq [\bar{\theta}_1, \bar{\theta}_2, \ldots, \bar{\theta}_N, p]^{\mathrm{T}} \\ \varphi(\pi) \triangleq [\varphi(\pi, \pi_1), \varphi(\pi, \pi_2), \ldots, \varphi(\pi, \pi_N), 1]^{\mathrm{T}} \end{cases} \tag{19}$$

Based on equation (19), considering the approximation error $\hat{\varpi}$, the actuate approximation for the unknown nonlinear function over a compact set $S_\pi \subseteq \mathbb{R}^n$ can be expressed by

$$\hat{Y}(\pi) = \hat{\theta}^{\mathrm{T}} \varphi(\pi) + \hat{\varpi} \tag{20}$$

The ideal weight value $\theta^*$ of equation (20) is given by

$$\theta^* = \arg \min_{\theta \in S_f} \left[ \sup_{\pi \in S_\pi} \left| \hat{Y}\left(\pi | (\hat{\theta})\right) - Y(\pi) \right| \right] \tag{21}$$

where $S_f = \{\hat{\theta} : |\hat{\theta}| \leq M_{\hat{\theta}}\}$ is a valid field of the estimate parameter $\hat{\theta}$ with $M_{\hat{\theta}}$ being a design parameter. Using the ideal weight value $\theta^*$ yields

$$Y(\pi) = \theta^{*\mathrm{T}} \varphi(\pi) + \varpi^*,\ |\varpi^*| \leq \varpi_{\max} \tag{22}$$

where $\varpi^*$ is the optimal approximation error and $\varpi_{\max}$ is the upper bound of $\varpi^*$.

**Remark 2.** Note that the newly defined weight $\theta$ in equation (19) is obtained by solving a linear function in equation (16) based on the first-order optimality conditions in equation (15). In this procedure, no optimization methods such as the quadratic programming method or the dynamic programming method, which are often applied to NN-based approximation, are needed. Namely, only two design parameters $c_0$ and $\zeta$ are required in the estimation for unknown nonlinear functions. Hence, this simplifies the optimization of the weight $\theta$ in the nonlinear approximation dramatically and is suitable for the online estimation of unknown hypersonic dynamics. Besides, it can be seen from equations (16) and (17) that the value of $\theta$ is globally optimal in the LS-SVM, which bypasses local minima during the training process. Moreover, when small-scale training samples ($N$ is small) are chosen, high confidence levels of the approximation can be obtained as well according to Vapnik and Suykens and Vandewalle.[17,18] Thus, it is advantageous to adopt the LS-SVM to approximate the unknown nonlinearities in equations (3) and (5) so the HFV benefits from its attractive computational property.

Based on the model description and preliminaries above, in what follows, two LS-SVM-based adaptive controllers under a TPPF are designed for velocity and altitude subsystems, respectively.

## LS-SVM-based adaptive controller design

Before devising the LS-SVM-based adaptive controllers under a TPPF, a control saturation approximation and a newly developed FTCD based on a hyperbolic tangent sigmoid function (HTSF) are given. A HTSF often works as a transfer function in a NN owing to its good properties such as mapping the large input into the small domain $(-1, 1)$.

### *Saturation approximation based on HTSF*

For the asymmetric or symmetric control saturations in equation (3), it is easy to find that there exists a sharp corner between the applied control $[\delta_e, \Phi]$ and the control input $[v_{\delta_e}, v_\Phi]$ when $v_{\delta_e} = u_{M1}^+ (\text{or } u_{M1}^-)$, $v_\Phi = u_{M2}^+ (\text{or } u_{M2}^-)$. Hence, the classical backstepping technique cannot be directly applied in the relevant controller design. In order to attenuate the negative effect induced by the sharp corner, the applied control $[\delta_e, \Phi]$ can be approximated by the HTSF in a general form like

$$\begin{cases} u = sat(v) = u_1 + u_2 \\ u_1 = \iota_0 \phi\left(\iota_1 (v - \iota_2)\right) + \iota_2 \\ \phi\left(\iota_1 (v - \iota_2)\right) = \dfrac{2}{1 + e^{-2 * \iota_1 (v - \iota_2)}} - 1 \\ \iota_0 = (u_M^+ - u_M^-)/2,\ \iota_2 = (u_M^+ + u_M^-)/2 \end{cases} \tag{23}$$

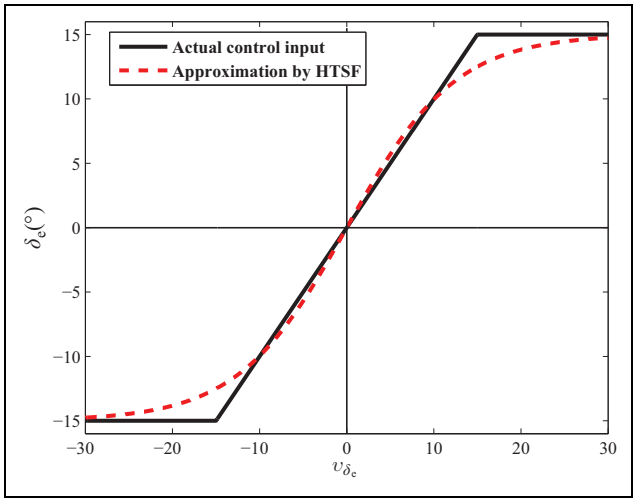


**Figure 1.** Saturation approximation for $\delta_e$ ($\iota_1 = 0.08$).

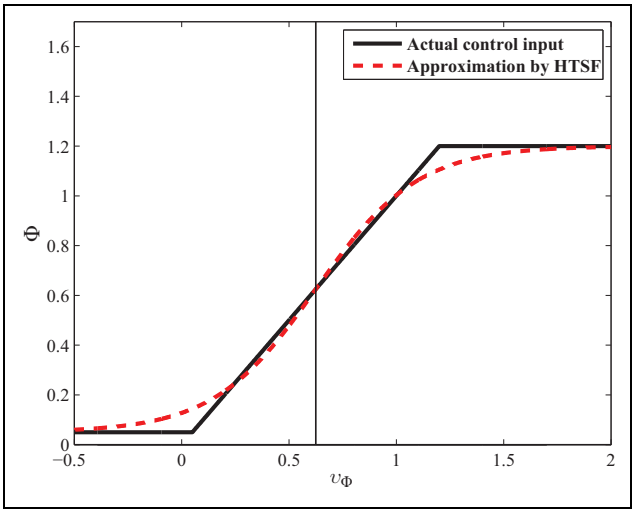


**Figure 2.** Saturation approximation for $\Phi$ ($\iota_1 = 2.1$).

where $\iota_1 \in (0, \infty)$ is a positive design constant determining the approximation accuracy. $u_1$ is the approximation term of the saturated control $u$. $u_2$ represents the approximation error. $v$, $u_M^+$, and $u_M^-$ have similar concepts with ones in equation (3). Along equation (23), the bound of the approximation error $u_2$ is restricted to

$$\begin{aligned} |u_2| &= |u - u_1| = |sat(v) - u_1| \\ &= \left| sat(v) - \left( \iota_0 \frac{2}{1 + e^{-2*\iota_1(v-\iota_2)}} + \iota_2 - \iota_0 \right) \right| \\ &\le (u_M^+ - u_M^-) \left( 1 - \frac{1}{1 + e^{-2*\iota_1(u_M^- - \iota_2)}} \right) \triangleq e u_{\max} \end{aligned} \tag{24}$$

In our work, considering the practical actuator constrains of a HFV, $\delta_e \in [-15^\circ, 15^\circ]$, $\Phi \in [0.05, 1.2]$,[11] the relevant approximations are given in Figures 1 and 2.

As portrayed in Figures 1 and 2, the saturation approximation errors by the HTSF are bounded. And by adjusting the parameter $\iota_1$, the approximation error can be made arbitrarily small.

## Novel finite-time-convergent differentiator

A novel FTCD with a simple structure is developed using the HTSF in this part. The newly developed FTCD (labeled as hyperbolic finite-time-convergent differentiator [HFTCD]) has two good properties as follows.

1. The structure of the HFTCD is comparatively simple and can track the desired signal and its high-order derivatives accurately with global asymptotic stability within a finite time.
2. In the estimation for the desired signal, a good dynamic response and high accuracy can be obtained using the HFTCD. Besides, the chattering near the trim point is weakened, or even eliminated, under the proposed HFTCD.

Prior to the design of HFTCD, some necessary concepts are given.

**Definition 1.**[31,34] Consider a time-invariant autonomous system expressed by

$$\dot{\chi} = \hbar(\chi), \quad \hbar(0) = 0, \quad \chi = [\chi_1, \chi_2, \ \cdots \ , \chi_n]^{\mathrm{T}} \in \mathbb{R}^n \tag{25}$$

where $\hbar : S_\chi \to \mathbb{R}^n$ is continuous on an open neighborhood $S_{\chi 0}$ of the origin $(0, 0)$. Without loss of generality, the origin $[0]_{n\times 1}$ is assumed to be the trim point of the system given by equation (25) and the finite-time stability is obtained if:

(a) it is asymptotically stable in $S_\chi$ with $S_\chi \subseteq S_{\chi 0}$;
(b) it is finite-time convergent in $S_\chi$, that is, there exists a setting time $T_s > 0$ such that every solution $\chi(t)$ of the system given by equation (25) is kept on $S_\chi \backslash \{0\}$ for any initial condition $\chi(0) \in S_\chi \backslash \{0\}$; and for all $t \in [0, \infty)$, it satisfies

$$\lim_{t \to T_s} \chi(t) = 0, \ \text{ and } \chi(t) = 0, \ \forall t \in [T_s, \ +\infty) \tag{26}$$

Note that when $S_\chi = \mathbb{R}^n$, the system given by equation (25) is globally finite-time stable at the origin when satisfying the aforementioned conditions.

**Lemma 1.** *(Bhat and Bernstein[32]) Suppose there exists a positively continuous function $J_1 : S_{\chi 0} \to \mathbb{R}$ satisfying the following condition*

$$\dot{J}_1(\chi) + \Im\left(J_1(\chi)\right)^\vartheta \le 0, \ \ \chi \in S_\chi \subseteq S_{\chi 0} \backslash \{0\} \tag{27}$$

*where $\Im > 0$, $\vartheta \in (0, 1)$ are constants. The rest of the parameters are the same as the ones in Definition 1. Then the system given by equation (25) is finite-time stable at the origin and the setting time $T_s$ satisfies*

$$T_s \le \frac{1}{\Im(1 - \vartheta)} (J_1(\chi))^{1-\vartheta} \tag{28}$$

Apart from the aforementioned definition and lemma, some necessary and useful assumptions are given.

**Assumption 1.** Given that the smooth function $\hbar(\chi)$ satisfies

$$|\hbar(\tilde{\chi}_1, \tilde{\chi}_2, \ldots, \tilde{\chi}_n) - \hbar(\bar{\chi}_1, \bar{\chi}_2, \ldots, \bar{\chi}_n)| \leq c_1 \sum_{i=1}^{n} |\tilde{\chi}_i - \bar{\chi}_i|^{\varsigma},\ c_1 > 0,\ \varsigma \in (0, 1] \tag{29}$$

where $c_1$ and $\varsigma$ are constants. Besides, the positively continuous function $J_1$ is Lipschitz with a Lipschitz constant $M_c$.

Based on the previous discussions, construct the following system in the form of

$$\begin{cases} \dot{\chi}_i = \chi_{i+1},\ i = 1, 2, \ldots, n-1 \\ \dot{\chi}_n = \hbar(\chi_1, \chi_2, \ldots, \chi_n) = -\lambda_1 \phi(\ell_1 \chi_1) - \lambda_2 \phi(\ell_2 \chi_2) - \cdots - \lambda_n \phi(\ell_n \chi_n) \end{cases} \tag{30}$$

where $\chi = [\chi_1, \chi_2, \ldots, \chi_n] \in S_\chi$. $\lambda_i$, $\ell_i\,(i = 1, 2, \ldots, n)$ are the positive design constants.

**Theorem 1.** *When the Lyapunov function candidate incorporating with the continuous function $\hbar$ is chosen as*

$$\begin{cases} J_1 = \int_0^{\chi_1} \lambda_1 \phi(\ell_1 \tau) d\tau + \int_{\chi_1}^{\chi_2} \omega_2 \phi(\ell_2 \tau) d\tau + \cdots + \int_{\chi_{n-2}}^{\chi_{n-1}} \omega_{n-1} \phi(\ell_{n-1} \tau) d\tau + \chi_n^2 + c_2 \\ 0 < \chi_1 < \chi_2 < \cdots < \chi_n < \chi_{\max},\ \omega_{i+1} = \max\{\lambda_1, \ldots, \lambda_{i+1}\},\ \ell_i \leq \ell_{i+1},\ c_2 \geq 1,\ i = 1, 2, \ldots, n-2 \end{cases} \tag{31}$$

*where $\chi_{\max}$ is a positive constant, the system given by equation (30) is finite-time stable and the setting time $T_s$ satisfies the inequality given by equation (30).*

**Proof.** Taking time derivative of $J_1$ and we can obtain

$$\begin{aligned} \dot{J}_1 &= \lambda_1 \phi(\ell_1 \chi_1) \dot{\chi}_1 + (\omega_2 \phi(\ell_2 \chi_2) \dot{\chi}_2 - \omega_2 \phi(\ell_2 \chi_1) \dot{\chi}_1) + \cdots + (\omega_{n-1} \phi(\ell_{n-1} \chi_{n-1}) \dot{\chi}_{n-1} - \omega_{n-1} \phi(\ell_{n-1} \chi_{n-2}) \dot{\chi}_{n-2}) + 2\chi_n \dot{\chi}_n \\ &= (\lambda_1 \phi(\ell_1 \chi_1) - \omega_2 \phi(\ell_2 \chi_1)) \dot{\chi}_1 + (\omega_2 \phi(\ell_2 \chi_2) - \omega_3 \phi(\ell_3 \chi_2)) \dot{\chi}_2 + \cdots + \omega_{n-1} \phi(\ell_{n-1} \chi_{n-1}) \dot{\chi}_{n-1} + 2\chi_n \dot{\chi}_n \\ &\leq \omega_{n-1} \phi(\ell_{n-1} \chi_{n-1}) \dot{\chi}_{n-1} + 2\chi_n \dot{\chi}_n \\ &= \omega_{n-1} \phi(\ell_{n-1} \chi_{n-1}) \chi_n + 2\chi_n (-\lambda_1 \phi(\ell_1 \chi_1) - \lambda_2 \phi(\ell_2 \chi_2) - \cdots - \lambda_{n-1} \phi(\ell_{n-1} \chi_{n-1}) - \lambda_n \phi(\ell_n \chi_n)) \\ &\leq -\lambda_1 \phi(\ell_1 \chi_1) \chi_n - \lambda_2 \phi(\ell_2 \chi_2) \chi_n - \cdots - \lambda_{n-1} \phi(\ell_{n-1} \chi_{n-1}) \chi_n - \lambda_n \phi(\ell_n \chi_n) \chi_n \\ &\leq -\lambda_1 \phi(\ell_1 \chi_1) \chi_1 - \lambda_2 \phi(\ell_2 \chi_2) \chi_2 - \cdots - \lambda_n \phi(\ell_n \chi_n) \chi_n \end{aligned} \tag{32}$$

Employing the "mean value theorem of integrals", the following inequalities can be obtained

$$\begin{aligned} &\int_0^{\chi_1} \lambda_1 \phi(\ell_1 \tau) d\tau \leq \lambda_1 \phi(\ell_1 \chi_1) \chi_1 \\ &\int_{\chi_i}^{\chi_{i+1}} \omega_{i+1} \phi(\ell_{i+1} \tau) d\tau \leq \omega_{i+1} \phi(\ell_{i+1} \chi_{i+1}) \chi_{i+1},\ i = 1, 2, \ldots, n-2 \end{aligned} \tag{33}$$

Along the inequalities given by equation (33), the inequality given by equation (32) becomes

$$\begin{cases} \dot{J}_1 \leq -\int_0^{\chi_1} \lambda_1 \phi(\ell_1 \tau) d\tau - \int_{\chi_1}^{\chi_2} \lambda_2 \phi(\ell_2 \tau) d\tau - \cdots - \int_{\chi_{n-2}}^{\chi_{n-1}} \lambda_{n-1} \phi(\ell_{n-1} \tau) d\tau \\ \quad = -J_1 + \Delta J_1 \\ \Delta J_1 = \int_{\chi_1}^{\chi_2} (\omega_2 - \lambda_2) \phi(\ell_2 \tau) d\tau + \cdots + \int_{\chi_{n-2}}^{\chi_{n-1}} (\omega_{n-1} - \lambda_{n-1}) \phi(\ell_{n-1} \tau) d\tau + \chi_n^2 + c_2 \geq 0 \end{cases} \tag{34}$$

It is easy to obtain $J_1 \geq 1$ based on equation (31). Invoking the inequality given by equation (34), there exist $\Im > 0$, $\vartheta \in (0, 1)$ and the following inequality holds

$$-J_1 + \Delta J_1 = -\Im (J_1)^{\vartheta} \tag{35}$$

Further, we can obtain

$$\dot{J}_1 + \Im (J_1)^{\vartheta} \leq 0 \tag{36}$$

According to Lemma 1, then the setting time $T_s$ satisfies the inequality given by equation (28). This completes the proof of Theorem 1.

Note that when $\chi_n < \chi_{n-1} < \cdots < \chi_1 < 0$, Theorem 1 holds as well. The process of the proof is similar to the previous one.

When $\hbar$ is chosen as the form of equation (30), Assumption 1 is satisfied and the relevant proof is as follows.

***Proof.*** Take time derivative of $\phi(\ell\chi)$

$$\begin{aligned} \frac{d\phi(\ell\chi)}{d\chi} &= \frac{d}{d\chi}\left(\frac{2}{1 + e^{-2\ell\chi}} - 1\right) = \frac{4\ell e^{-2\ell\chi}}{(1 + e^{-2\ell\chi})^2} \\ &\leq \ell \frac{(1 + e^{-2\ell\chi})^2}{(1 + e^{-2\ell\chi})^2} = \ell \end{aligned} \tag{37}$$

Then $\hbar$ satisfies

$$
\begin{aligned}
|\hbar(\tilde{\chi}_1,\tilde{\chi}_2,\ \ldots\ ,\tilde{\chi}_n)-\hbar(\bar{\chi}_1,\bar{\chi}_2,\ \ldots\ ,\bar{\chi}_n)| &= |\Big(\lambda_1\phi(\ell_1\bar{\chi}_1)-\lambda_1\phi(\ell_1\tilde{\chi}_1)\Big)+\Big(\lambda_2\phi(\ell_2\bar{\chi}_2)-\lambda_2\phi(\ell_2\tilde{\chi}_2)\Big)+\cdots \\
&\quad+\Big(\lambda_n\phi(\ell_n\bar{\chi}_n)-\lambda_n\phi(\ell_n\tilde{\chi}_n)\Big)| \\
&\le \lambda_1|\phi(\ell_1\bar{\chi}_1)-\phi(\ell_1\tilde{\chi}_1)|+\lambda_2|\phi(\ell_2\bar{\chi}_2)-\phi(\ell_2\tilde{\chi}_2)|+\cdots+\lambda_n|\phi(\ell_n\bar{\chi}_n)-\phi(\ell_n\tilde{\chi}_n)| \\
&\le \lambda_1\ell_1|\tilde{\chi}_1-\bar{\chi}_1|+\lambda_2\ell_2|\tilde{\chi}_2-\bar{\chi}_2|+\cdots+\lambda_n\ell_n|\tilde{\chi}_n-\bar{\chi}_n| \\
&\le \lambda_{\max}\textstyle\sum_{i=1}^{n}|\tilde{\chi}_i-\bar{\chi}_i|,\ \lambda_{\max}=\max\{\lambda_1\ell_1,\lambda_2\ell_2,\ \ldots\ ,\lambda_n\ell_n\}
\end{aligned}
\tag{38}
$$

Thereby, the inequality given by equation (29) is satisfied when $\hbar$ is chosen as the form of equation (30). Consequently, it is easy to prove that $J_1$ is Lipschitz.

In order to obtain the HFTCD, the bounded and integrable input signal $\wp(t)$ should satisfy the following the assumption.

**Assumption 2.**[33] The bounded and integrable input signal $\wp(t)$ has $(n-2)$-order derivative on the whole time domain. At some time instants, its $(n-1)$-order derivative may not exists, but its $(n-1)$-order left and right derivatives exist and do not equal.

**Theorem 2.** *When Assumptions 1 and 2 hold, based on Theorem 1, the following system*

$$
\begin{cases}
\dot{\xi}_i=\xi_{i+1},\ i=1,2,\ \ldots\ ,n-1 \\
\dot{\xi}_n=-R^n\left(\lambda_1\phi\Big(\ell_1(\xi_1-\wp)\Big)+\lambda_2\phi\left(\dfrac{\ell_2\xi_2}{R}\right)+\cdots+\lambda_n\phi\left(\dfrac{\ell_n\xi_n}{R^{n-1}}\right)\right)
\end{cases}
\tag{39}
$$

*is finite-time stable and there exist* $\sigma>0,\ \tilde{\lambda}_1\sigma>n$ *such that* $\xi_i-\wp^{i-1}=O\Big((1/R)^{\tilde{\lambda}_1\sigma-i+1}\Big)\ (i=1,2,\ \ldots\ ,n)\ \ \sigma=\frac{1-\tilde{\lambda}_2}{\tilde{\lambda}_2}$, $\tilde{\lambda}_2\in(0,\ \tilde{\lambda}_{20}),\ \tilde{\lambda}_{20}=\min\Big\{\frac{\tilde{\lambda}_1}{\tilde{\lambda}_1+n},\ \frac{1}{2}\Big\},\ \forall n\ge 2$, *where R is a positive design constant and the rest of the parameters are the same as ones in Theorem 1.* $O\Big((1/R)^{\tilde{\lambda}_1\sigma-i+1}\Big)$ *represents the relevant high-order approximation error.*

**Proof.** Invoking Theorem 1 above, and according to Theorem 1 in the work by Bu et al. and Wang et al.,[28,33] it is easy to conclude that Theorem 2 holds.

**Remark 3.** Theorem 2 gives the detailed form of the HFTCD and equation (39) reveals that $\lim_{R\to+\infty}(\xi_i-\wp^{i-1})=0,\ \forall i=1,2,\ \ldots\ ,n$. Practically, $\wp^{i-1}$ can be estimated precisely under appropriate parameter $R$. Further, one can conclude that the HFTCD has the properties mentioned at beginning of this subsection.

## *LS-SVM-based adaptive controller subject to actuator saturation for the velocity subsystem*

For the velocity subsystem given by equation (3), under the TPPF in equation (6), the transformed error of the velocity tracking error $\tilde{V}$ can be obtained based on equation (10) expressed by

$$
s_V=\frac{1}{2}\ln\left(\frac{\delta_{V1}+\Lambda_V}{\delta_{V2}-\Lambda_V}\right),\ \Lambda_V=\frac{\tilde{V}}{\mu_V}
\tag{40}
$$

The derivative of $s_V$ is

$$
\begin{aligned}
\dot{s}_V &= \frac{\partial s_V(t)}{\partial\Lambda_V}\frac{d\Lambda_V}{dt}+\frac{\partial s_V(t)}{\partial\delta_{V1}}\frac{d\delta_{V1}}{dt}+\frac{\partial s_V(t)}{\partial\delta_{V2}}\frac{d\delta_{V2}}{dt} \\
&= \varepsilon_V(f_V+\Phi-\dot{V}_r-\Lambda_V\dot{\mu}_V+\delta_V/\varepsilon_V)
\end{aligned}
\tag{41}
$$

where $\varepsilon_V=\frac{1}{2\mu_V}\left(\frac{1}{\delta_{V1}+\Lambda_V}+\frac{1}{\delta_{V2}-\Lambda_V}\right)$ and $\delta_V=\frac{1}{2}\left(\frac{1}{\delta_{V1}+\Lambda_V}\dot{\delta}_{V1}-\frac{1}{\delta_{V2}-\Lambda_V}\dot{\delta}_{V2}\right)$. $\delta_{V1}$, $\delta_{V2}$ and $\mu_V$ are design smooth decaying functions. The unknown nonlinearity $f_V$ in equation (41) can be estimated by a LS-SVM-based approximator according to equation (22)

$$
f_V=\theta_V^{*\mathrm{T}}\phi(\bar{V})+\varpi_1^*,\ |\varpi_1^*|\le\varpi_{1\max},\ \|\theta_V^*\|^2\le\theta_{V\max}
\tag{42}
$$

where $\bar{V}=[T,D,\alpha,\gamma,\Phi]$. $\theta_V^*\in\mathbb{R}^{N_1+1}$ and $\varpi_1^*\in\mathbb{R}$ are, respectively, the ideal weight and the approximation error with $N_1$ being the total number of training samples of the LS-SVM. To reduce the complexity of the online adaptation of $(N_1+1)$-dimensional weight $\theta_V^*$, alternatively, define $\eta_V^*=\|\theta_V^*\|^2$ as the new estimation parameter. Herein, only one scalar needs to be reduced online which drops the computational load dramatically.

For compensating the input saturation of the fuel equivalence ratio, defining $e_V=s_V-s_{V0}$ with $s_{V0}$ being an auxiliary state, a new system can be formed as

$$
\begin{aligned}
\dot{e}_V &= \dot{s}_V-\dot{s}_{V0}=\varepsilon_V(f_V+s_{V0}-\dot{V}_r-\Lambda_V\dot{\mu}_V+\delta_V/\varepsilon_V+v_\Phi) \\
&= \varepsilon_V\Big(\theta_1^{*\mathrm{T}}\varphi(\bar{V})+\varpi_1^*+s_{V0}-\dot{V}_r-\Lambda_V\dot{\mu}_V+\delta_V/\varepsilon_V+v_\Phi\Big)
\end{aligned}
\tag{43}
$$

with

$$\dot{s}_{V0} = -\varepsilon_V s_{V0} + \varepsilon_V(sat(v_\Phi) - v_\Phi) \tag{44}$$

Note that $\varepsilon_V > 0$ holds in the whole time domain. When the newly defined system state $e_V$ is bounded, considering the boundedness of $s_{V0}$, $s_V$ can preserve its transient and steady-state performance defined by TPPF in equation (40). Therefore, the task of the velocity subsystem is to design an appropriate control input $v_\Phi$ to shrink the newly defined error $e_V$ to a small domain. The LS-SVM-based adaptive controller $v_\Phi$ is devised as

$$\begin{aligned} v_\Phi = &-k_{V1}e_V - k_{V2}\int_0^t e_V(\tau)d\tau + \dot{V}_r - \ell_{V1}e_V\hat{\eta}_V\varphi^{\mathrm{T}}(\bar{V})\varphi(\bar{V}) \\ &+ \ell_{V2}\hat{\eta}_V + \Lambda_V\dot{\mu}_V - \delta_V/\varepsilon_V - s_{V0} \end{aligned} \tag{45}$$

where $k_{V1}$, $k_{V2}$, $\ell_{V1}$, $\ell_{V2}$, and $\Gamma_V$ denote the positive design constants. $\hat{\eta}_V$ is the estimation of $\eta_V^*$, and its adaptive scheme is

$$\dot{\hat{\eta}}_V = \mathrm{Proj}\Big(\Gamma_V\Big(-\ell_{V2}e_V + \ell_{V1}e_V^2\varphi^{\mathrm{T}}(\bar{V})\varphi(\bar{V})\Big)\Big) \tag{46}$$

where the parameter projection $\mathrm{Proj}(\bullet)$ satisfies

$$\mathrm{Proj}_\Psi(\Xi) = \begin{cases} 0, & \text{if } \Psi = \Psi_{\min},\ \Xi < 0 \\ 0, & \text{if } \Psi = \Psi_{\max},\ \Xi > 0 \\ \Xi, & \text{otherwise} \end{cases} \tag{47}$$

Under the LS-SVM-based adaptive controller equation (45), the stability analysis of the system given by equation (43) is given as follows.

**Theorem 3.** *Consider the closed-loop system comprising of the plant equation (43) with the LS-SVM-based approximation for nonlinearity in equation (42), designed controller in equation (45), adaptive scheme in equation (46), then all the signals involved are bounded and the velocity tracking error can preserve its transient and steady-state performance defined by the TPPF in equation (40).*

**Proof.** Construct the following Lyapunov function candidate as

$$J_V = \frac{1}{2\varepsilon_V}e_V^2 + \frac{1}{2}k_{V2}\left(\int_0^t e_V(\tau)d\tau\right)^2 + \frac{1}{2\Gamma_V}\tilde{\eta}_V^2 \tag{48}$$

where $\tilde{\eta}_V = \hat{\eta}_V - \eta_V^*$. According to equations (44) to (47), the derivative of $J_V$ satisfies

$$\begin{aligned} \dot{J}_V &= \frac{1}{\varepsilon_V}e_V\dot{e}_V - \frac{\dot{\varepsilon}_V}{2\varepsilon_V^2}e_V^2 + k_{V2}e_V\int_0^t e_V(\tau)d\tau + \frac{1}{\Gamma_V}\tilde{\eta}_V\dot{\tilde{\eta}}_V \\ &= e_V\Big(\theta_V^{*\mathrm{T}}\varphi(\bar{V}) + \varpi_1^* + s_{V0} - \dot{V}_r - \Lambda_V\dot{\mu}_V + \delta_V/\varepsilon_V + v_\Phi\Big) - \frac{\dot{\varepsilon}_V}{2\varepsilon_V^2}e_V^2 + k_{V2}e_V\int_0^t e_V(\tau)d\tau + \frac{1}{\Gamma_V}\tilde{\eta}_V\dot{\tilde{\eta}}_V \\ &= -\left(k_{V1} + \frac{\dot{\varepsilon}_V}{2\varepsilon_V^2}\right)e_V^2 + e_V\theta_V^{*\mathrm{T}}\varphi(\bar{V}) - \ell_{V1}e_V^2\hat{\eta}_V\varphi^{\mathrm{T}}(\bar{V})\varphi(\bar{V}) + \ell_{V2}\hat{\eta}_V e_V + \frac{1}{\Gamma_V}\tilde{\eta}_V\dot{\tilde{\eta}}_V + e_V\varpi_1^* \\ &\le -\left(k_{V1} - \ell_{V1} + \frac{\dot{\varepsilon}_V}{2\varepsilon_V^2}\right)e_V^2 + \ell_{V1}e_V^2\eta_V^*\varphi^{\mathrm{T}}(\bar{V})\varphi(\bar{V}) - \ell_{V1}e_V^2\hat{\eta}_V\varphi^{\mathrm{T}}(\bar{V})\varphi(\bar{V}) + \frac{1}{\Gamma_V}\tilde{\eta}_V\dot{\tilde{\eta}}_V + \ell_{V2}\hat{\eta}_V e_V + \frac{1+\varpi_1^{*2}}{4\ell_{V1}} \\ &= -\left(k_{V1} - \ell_{V1} + \frac{\dot{\varepsilon}_V}{2\varepsilon_V^2}\right)e_V^2 - \ell_{V1}e_V^2\tilde{\eta}_V\varphi^{T}(\bar{V})\varphi(\bar{V}) + \ell_{V2}\tilde{\eta}_V e_V + \ell_{V2}\eta_V^* e_V + \frac{1}{\Gamma_V}\tilde{\eta}_V\dot{\tilde{\eta}}_V + \frac{1+\varpi_1^{*2}}{4\ell_{V1}} \\ &= -\left(k_{V1} - \ell_{V1} + \frac{\dot{\varepsilon}_V}{2\varepsilon_V^2}\right)e_V^2 - \tilde{\eta}_V\Im_V + \tilde{\eta}_V\left(\frac{1}{\Gamma_V}\mathrm{Proj}(\Gamma_V\Im_V)\right) + \ell_{V2}\eta_V^* e_V + \frac{1+\varpi_1^{*2}}{4\ell_{V1}} \\ &= -\left(k_{V1} - \ell_{V1} + \frac{\dot{\varepsilon}_V}{2\varepsilon_V^2}\right)e_V^2 - \tilde{\eta}_V\left(\Im_V - \frac{1}{\Gamma_V}\mathrm{Proj}(\Gamma_V\Im_V)\right) + \ell_{V2}\eta_V^* e_V + \frac{1+\varpi_1^{*2}}{4\ell_{V1}} \\ &\le -\left(k_{V1} - \ell_{V1} - \ell_{V2} + \frac{\dot{\varepsilon}_V}{2\varepsilon_V^2}\right)e_V^2 + \frac{\ell_{V2}\eta_V^{*2}}{4} + \frac{1+\varpi_{1\max}^2}{4\ell_{V1}} \\ &\le -\bar{k}_{V1}e_V^2 + \frac{\ell_{V2}\eta_V^{*2}}{4} + \frac{1+\varpi_{1\max}^2}{4\ell_{V1}} \end{aligned} \tag{49}$$

where $\bar{k}_{V1} \triangleq k_{V1} - \ell_{V1} - \ell_{V2} + \dot{\varepsilon}_V/(2\varepsilon_V^2)$, $\Im_V \triangleq -\ell_{V2}e_V + \ell_{V1}e_V^2\varphi^{\mathrm{T}}(\bar{V})\varphi(\bar{V})$. Let $k_{V1} > \max\{\ell_{V1} + \ell_{V2} - \dot{\varepsilon}_V/(2\varepsilon_V^2)\}$, then $e_V$ is invariant to the following set

$$\Omega_{e_V} = \left\{ e_V \middle| |e_V| \le \sqrt{\left(\frac{\ell_{V2}\eta_V^{*2}}{4} + \frac{1+\varpi_{1\max}^{*2}}{4\ell_{V1}}\right)/\bar{k}_{V1}} \right\} \tag{50}$$

When a sufficiently large $\bar{k}_{V1}$ is chosen, the radius of $\Omega_{e_V}$ can be made arbitrarily small. According to the inequalities given by equations (49) and (50), it can be seen that the designed adaptive controller in equation (45) can steer the newly defined state $e_V$ to a small invariant stably. This guarantees $e_V$ and $s_{V0}$ are bounded. Thereby, the velocity tracking error $\tilde{V}$ can preserve its transient and steady-state performance defined by TPPF. This completes the proof of Theorem 3.

### LS-SVM-based adaptive controller subject to actuator saturation for the altitude subsystem

As for the tracking control for altitude subsystem, under the TPPF in equation (6), the transformed error of the altitude tracking error $\tilde{h}$ can be obtained based on equation (10) expressing by

$$s_h = \frac{1}{2}\ln\left(\frac{\delta_{h1}+\Lambda_h}{\delta_{h2}-\Lambda_h}\right),\ \Lambda_h = \frac{\tilde{h}}{\mu_h} \tag{51}$$

Along equations (1) and (51), take the derivative of $s_h$ as

$$\begin{aligned}\dot{s}_h &= \frac{\partial s_h(t)}{\partial \Lambda_h}\frac{d\Lambda_h}{dt} + \frac{\partial s_h(t)}{\partial \delta_{h1}}\frac{d\delta_{h1}}{dt} + \frac{\partial s_h(t)}{\partial \delta_{h2}}\frac{d\delta_{h2}}{dt} \\ &= \varepsilon_h(V\sin\gamma - \dot{h}_r - \Lambda_h\dot{\mu}_h + \delta_h/\varepsilon_h)\end{aligned} \tag{52}$$

with $\varepsilon_h = \frac{1}{2\mu_h}\left(\frac{1}{\delta_{h1}+\Lambda_h} + \frac{1}{\delta_{h2}-\Lambda_h}\right)$ and $\delta_h = \frac{1}{2}\left(\frac{1}{\delta_{h1}+\Lambda_h}\dot{\delta}_{h1} - \frac{1}{\delta_{h2}-\Lambda_h}\dot{\delta}_{h2}\right)$, where $\delta_{h1}$, $\delta_{h2}$, and$\mu_h$ are design smooth decaying functions. Then define the command of $\gamma_d$ as

$$\gamma_d = \frac{-k_{h1}s_h - k_{h2}\int_0^t s_h(\tau)d\tau + \dot{h}_r + \Lambda_h\dot{\mu}_h - \delta_h/\varepsilon_h}{V} \tag{53}$$

with

$$\dot{\gamma}_d \approx \frac{-k_{h1}\dot{s}_h - k_{h2}s_h + \ddot{h}_r + \Lambda_h\ddot{\mu}_h + \dot{\Lambda}_h\dot{\mu}_h - (\dot{\delta}_h\varepsilon_h - \delta_h\dot{\varepsilon}_h)/\varepsilon_h^2}{V} \tag{54}$$

where $k_{h1}$ and $k_{h2}$ are positive design constants. As discussed in the 'Problem statement and preliminaries' section, when $\gamma$ can track the given command $\gamma_d$, then the altitude tracking error $\tilde{h}$ can be regulated to zero stably while preserving its transient and steady-state performance depicted in equation (51). When tracking the given command $\gamma_d$ defined in equation (53), two problems encountered in equation (5) should be addressed ahead of designing the relevant controller. One is the observation of the newly defined state variables $z_2$ and $z_3$. Another is the estimation of $a(\bar{x}_3)$.

For the first problem, according to Theorem 2, the newly developed HFTCD can be applied to obtain the estimation for $z_2$ and $z_3$ in the following form

$$\begin{cases}\dot{\xi}_i = \xi_{i+1},\ i = 1,2 \\ \dot{\xi}_3 = -R^3(\lambda_{h1}\phi(\ell_{h1}(\xi_1 - z_1)) + \lambda_{h2}\phi(\ell_{h2}\xi_2/R) + \lambda_{h3}\phi(\ell_{h3}\xi_3/R^2))\end{cases} \tag{55}$$

where $R$, $\lambda_{hi}$, and $\ell_{hi}$ $(i = 1,2,3)$ are positive design constants, and $\ell_{hi}$ satisfies the condition given in Theorem 1. The estimation errors for $z_2$ and $z_3$ refer to Theorem 2. Then the tracking error based on equation (5) and the HFTCD-based tracking error based on equation (55) for $\gamma$ can be obtained as

$$\begin{cases} e \triangleq [e_1, e_2, e_3] = [z_1 - \gamma_d, z_2 - \dot{\gamma}_d, z_3 - \ddot{\gamma}_d] \\ \hat{e} \triangleq [\hat{e}_1, \hat{e}_2, \hat{e}_3] = [\xi_1 - \gamma_d, \xi_2 - \dot{\gamma}_d, \xi_3 - \ddot{\gamma}_d] \\ \tilde{e} \triangleq \hat{e} - e = [0, \tilde{e}_2, \tilde{e}_3] \end{cases} \tag{56}$$

Note that the tracking error of the initial system (5) for $\gamma$ is not changed considering $\xi_1 = z_1 = y_h$.

According to equation (56), the corresponding error system is constructed in the following form based on the backstepping technique.

**Step 1.** Define $e_{h1} = e_1$ and take its derivative as

$$\dot{e}_{h1} = \dot{\xi}_1 - \dot{\gamma}_d - \tilde{e}_2 = e_{h2} + v_{d1} - \dot{\gamma}_d - \tilde{e}_2 \tag{57}$$

by defining $e_{h2} = \xi_2 - v_{d1}$ with $v_{d1}$ being the virtual control term. Design the virtual control as $v_{d1} = -k_{\gamma 1}e_{h1} + \dot{\gamma}_d$ with $k_{\gamma 1}$ being a positive design constant. Then equation (60) equals to

$$\dot{e}_{h1} = -k_{\gamma 1}e_{h1} + e_{h2} - \tilde{e}_2 \tag{58}$$

Construct the following Lyapunov function candidate as

$$J_{h1} = \frac{1}{2}e_{h1}^2 \tag{59}$$

Based on equation (59), the derivative of $J_{h1}$ satisfies

$$\begin{aligned}\dot{J}_{h1} &= e_{h1}\dot{e}_{h1} = e_{h1}(-k_{\gamma 1}e_{h1} + e_{h2} - \tilde{e}_2) \\ &\le -(k_{\gamma 1} - 1)e_{h1}^2 + e_{h1}e_{h2} + \frac{1}{4}\tilde{e}_2^2 \\ &= -\bar{k}_{\gamma 1}e_{h1}^2 + e_{h1}e_{h2} + O_{h1}\end{aligned} \tag{60}$$

where $\bar{k}_{\gamma 1} \triangleq k_{\gamma 1} - 1 > 0$ and $O_{h1} \triangleq \tilde{e}_2^2/4$.

**Step 2.** Define $e_{h3} = \xi_3 - v_{d2} - e_{h0}$ with $v_{d2}$ and $e_{h0}$ being, respectively, the virtual control term and the auxiliary state given later. The derivative of $e_{h2}$ is

$$\dot{e}_{h2} = \dot{\xi}_2 - \dot{v}_{d1} = e_{h3} + v_{d2} + e_{h0} - \dot{v}_{d1} \tag{61}$$

Devise the virtual control $v_{d2}$ as

$$v_{d2} = -k_{\gamma 2} e_{h2} + \dot{v}_{d1} - e_{h1} - e_{h0} \tag{62}$$

where $k_{\gamma 2}$ is a positive design constant. In order to avoid intricate analysis and computation for $\dot{v}_{d1}$ containing $\ddot{\gamma}_d$ and $\dot{v}_{d1}$ can be estimated by a two-order HFTCD proposed above in the following form

$$\begin{cases} \dot{\chi}_{11} = \chi_{12} \\ \dot{\chi}_{12} = -R_{11}^2(\lambda_{11}\phi(\ell_{11}(\chi_{11} - v_{d1})) + \lambda_{12}\phi(\ell_{12}\chi_{12}/R_{11})) \end{cases} \tag{63}$$

where $R_{11}$, $\lambda_{1i}$, and $\ell_{1i}(i = 1, 2)$ are positive design constants. According to Theorem 2, $\chi_{12} - \dot{v}_{d1} = O\left((1/R_{11})^{\bar{\lambda}_{11}\sigma_{11}-i+1}\right) \triangleq O_{12}$. Then $v_{d2} = -k_{\gamma 2} e_{h2} + \chi_{12} - e_{h1} - e_{h0}$ and equation (60) equals to

$$\dot{e}_{h2} = -k_{\gamma 2} e_{h2} - e_{h1} + e_{h3} + O_{12} \tag{64}$$

Construct the following Lyapunov function candidate as

$$J_{h2} = \frac{1}{2} e_{h2}^2 \tag{65}$$

Based on equation (64), the derivative of $J_{h2}$ satisfies

$$\begin{aligned} \dot{J}_{h2} &= e_{h2}\dot{e}_{h2} = e_{h2}(-k_{\gamma 2} e_{h2} - e_{h1} + e_{h3} + O_{12}) \\ &\leq -(k_{\gamma 2} - 1)e_{h2}^2 - e_{h1}e_{h2} + e_{h2}e_{h3} + \frac{1}{4}O_{12}^2 \\ &= -\bar{k}_{\gamma 2} e_{h2}^2 - e_{h1}e_{h2} + e_{h2}e_{h3} + O_{h2} \end{aligned} \tag{66}$$

where $\bar{k}_{\gamma 2} \triangleq k_{\gamma 2} - 1 > 0$, $O_{h2} \triangleq O_{12}^2/4$.

**Step 3.** $e_{h3} = \xi_3 - v_{d2} - e_{h0}$. When the unknown nonlinearity is estimated by a LS-SVM-based approximator in equation (22), then the derivative of $e_{h3}$ can be written as

$$\begin{aligned} \dot{e}_{h3} &= \dot{\xi}_3 - \dot{v}_{d2} - \dot{e}_{h0} = a(\bar{x}_3) + \delta_e + O_3 - \dot{v}_{d2} - \dot{e}_{h0} \\ &= \theta_h^{*\mathrm{T}}\varphi(\bar{h}) + \varpi_2^* + \delta_e + O_3 - \dot{v}_{d2} - \dot{e}_{h0} \end{aligned} \tag{67}$$

with an auxiliary system for compensating the saturation of elevator deflection

$$\dot{e}_{h0} = -e_{h0} + \mathrm{sat}(v_{\delta_e}) - v_{\delta_e} \tag{68}$$

where $O_3$ is the approximation error between $\dot{\xi}_3$ and $\dot{z}_3$. $\theta_h^* \in \mathbb{R}^{N_2+1}$ is the ideal weight with $N_2$ being the total number of training samples of LS-SVM. $\bar{h} = \bar{x}_3$. Similarly, $\dot{v}_{d2}$ is estimated by a two-order HFTCD in the following form

$$\begin{cases} \dot{\chi}_{21} = \chi_{22} \\ \dot{\chi}_{22} = -R_{22}^2(\lambda_{21}\phi(\ell_{21}(\chi_{21} - v_{d2})) + \lambda_{22}\phi(\ell_{22}\chi_{22}/R_{22})) \end{cases} \tag{69}$$

where $R_{22}$, $\lambda_{2i}$, and $\ell_{2i}(i = 1, 2)$ are positive design constants. Based on Theorem 2, the estimation error satisfies $\chi_{22} - \dot{v}_{d2} = O\left((1/R_{22})^{\bar{\lambda}_{22}\sigma_{22}-i+1}\right) \triangleq O_{22}$. Then along equation (68), equation (67) equals to

$$\dot{e}_{h3} = \theta_h^{*\mathrm{T}}\varphi(\bar{h}) + e_{h0} + v_\delta - \chi_{22} + \varpi_2^* + O_{c3} \tag{70}$$

with $O_{c3} \triangleq O_3 + O_{22}$. Likewise, for reducing the complexity of regulating $(N_2 + 1)$-dimensional ideal weight $\theta_h^*$, defining $\eta_h^* = \|\theta_h^*\|^2$, then only one parameter needs to be updated adaptively online.

Based on equation (70), the actual LS-SVM-based adaptive controller $v_{\delta_e}$ is devised as

$$v_{\delta_e} = -k_{\gamma 3} e_{h3} - \ell_{\gamma 1} e_{h3}\hat{\eta}_h\varphi^{\mathrm{T}}(\bar{h})\varphi(\bar{h}) + \ell_{\gamma 2}\hat{\eta}_h + \chi_{22} - e_{h0} - e_{h2} \tag{71}$$

where $k_{\gamma 3}$, $\ell_{\gamma 1}$, and $\ell_{\gamma 2}$ are positive design constants. $\hat{\eta}_h$ is the estimation for $\eta_h^*$ and its corresponding adaptive scheme is

$$\dot{\hat{\eta}}_h = \mathrm{Proj}(\Gamma_h(-\ell_{\gamma 2} e_{h3} + \ell_{\gamma 1} e_{h3}^2\varphi^{\mathrm{T}}(\bar{h})\varphi(\bar{h}))) \tag{72}$$

where $\Gamma_h$ is a positive design constant. Substituting equation (70) into (69) yields

$$\begin{aligned} \dot{e}_{h3} = \theta_h^{*\mathrm{T}}\varphi(\bar{h}) - k_{\gamma 3} e_{h3} - \ell_{\gamma 1} e_{h3}\hat{\eta}_h\varphi^{\mathrm{T}}(\bar{h})\varphi(\bar{h}) + \ell_{\gamma 2}\hat{\eta}_h \\ - e_{h2} + \varpi_2^* + O_{c3} \end{aligned} \tag{73}$$

Then construct the following Lyapunov function candidate as

$$J_{h3} = \frac{1}{2} e_{h3}^2 + \frac{1}{2\Gamma_h}\tilde{\eta}_h^2 \tag{74}$$

where $\tilde{\eta}_h = \hat{\eta}_h - \eta_h^*$. Along equations (72) and (73), the derivative of $J_{h3}$ satisfies

$$\begin{aligned}
\dot{J}_{h3} &= e_{h3}\dot{e}_{h3} + \frac{1}{\Gamma_h}\tilde{\eta}_h\dot{\tilde{\eta}}_h \\
&= e_{h3}\left(\theta_h^{*\mathrm{T}}\varphi(\bar{h}) - k_{\gamma 3}e_{h3} - \ell_{\gamma 1}e_{h3}\hat{\eta}_h\varphi^{\mathrm{T}}(\bar{h})\varphi(\bar{h}) + \ell_{\gamma 2}\hat{\eta}_h - e_{h2} + \varpi_2^* + O_{c3}\right) + \frac{1}{\Gamma_h}\tilde{\eta}_h\dot{\tilde{\eta}}_h \\
&\le -(k_{\gamma 3} - \ell_{\gamma 1} - \ell_{\gamma 2})e_{h3}^2 + \ell_{\gamma 1}e_{h3}^2\eta_h^*\varphi^{\mathrm{T}}(\bar{h})\varphi(\bar{h}) - \ell_{\gamma 2}e_{h3}^2\hat{\eta}_h\varphi^{\mathrm{T}}(\bar{h})\varphi(\bar{h}) + \ell_{\gamma 2}\hat{\eta}_h e_{h3} - e_{h2}e_{h3} + \frac{1}{\Gamma_h}\tilde{\eta}_h\dot{\tilde{\eta}}_h \\
&\quad + \frac{1+\varpi_2^{*2}}{4\ell_{\gamma 1}} + \frac{1}{4\ell_{\gamma 2}}O_{c3}^2 \\
&\le -(k_{\gamma 3} - \ell_{\gamma 1} - \ell_{\gamma 2})e_{h3}^2 - \ell_{\gamma 1}e_{h3}^2\tilde{\eta}_h\varphi^{\mathrm{T}}(\bar{h})\varphi(\bar{h}) + \ell_{\gamma 2}\hat{\eta}_h e_{h3} + \frac{1}{\Gamma_h}\tilde{\eta}_h\dot{\hat{\eta}}_h + \frac{1+\varpi_{2\max}^2}{4\ell_{\gamma 1}} + \frac{1}{4\ell_{\gamma 2}}O_{c3}^2 - e_{h2}e_{h3} \\
&= -(k_{\gamma 3} - \ell_{\gamma 1} - \ell_{\gamma 2})e_{h3}^2 - \tilde{\eta}_h\Im_h + \tilde{\eta}_h\left(\frac{1}{\Gamma_h}\mathrm{Proj}(\Gamma_h\Im_h)\right) + \ell_{\gamma 2}\eta_h^* e_{h3} + \frac{1+\varpi_{2\max}^2}{4\ell_{\gamma 1}} + \frac{1}{4\ell_{\gamma 2}}O_{c3}^2 - e_{h2}e_{h3} \\
&\le -(k_{\gamma 3} - \ell_{\gamma 1} - 2\ell_{\gamma 2})e_{h3}^2 - \tilde{\eta}_h\left(\Im_h - \frac{1}{\Gamma_h}\mathrm{Proj}(\Gamma_h\Im_h)\right) + \frac{\ell_{\gamma 2}\eta_h^{*2}}{4} + \frac{1+\varpi_{2\max}^2}{4\ell_{\gamma 1}} + \frac{1}{4\ell_{\gamma 2}}O_{c3}^2 - e_{h2}e_{h3} \\
&= -\bar{k}_{\gamma 3}e_{h3}^2 + \frac{\ell_{\gamma 2}\eta_h^{*2}}{4} + \frac{1+\varpi_{2\max}^2}{4\ell_{\gamma 1}} - e_{h2}e_{h3} + O_{h3}
\end{aligned} \tag{75}$$

with $\bar{k}_{\gamma 3} \triangleq k_{\gamma 3} - \ell_{\gamma 1} - 2\ell_{\gamma 2} > 0$, $\Im_h \triangleq -\ell_{\gamma 2}e_{h3} + \ell_{\gamma 1}e_{h3}^2\varphi^{\mathrm{T}}(\bar{h})\varphi(\bar{h})$, and $O_{h3} \triangleq O_{c3}^2/4\ell_{\gamma 2}$. Based on aforementioned three steps, one of main results in this work is given as follows.

**Theorem 4.** *Consider the system consisting of the plants given by equations (4) and (5) with the HFTCD in equation (55) based on Theorem 2, the adaptation scheme of $\hat{\eta}_h$ in equation (72), the virtual control in euqtions (57) and (62) and the actual control in equation (71), all the signals involved are bounded with semi-global stability of the closed-loop system. Then, the altitude tracking error $\tilde{h}$ can achieve the time-varing predefined performance preplanned by the TPPF in equation (51) under actuator saturation.*

***Proof.*** Construct the following Lyapunov function candidate as

$$J_h = J_{h1} + J_{h2} + J_{h3} \tag{76}$$

Invoking the inequalities given by equations (60), (66) and (75), the derivative of $J_h$ satisfies

$$\begin{aligned}
\dot{J}_h &\le -\bar{k}_{\gamma 1}e_{h1}^2 + e_{h1}e_{h2} + O_{h1} - \bar{k}_{\gamma 2}e_{h2}^2 - e_{h1}e_{h2} + e_{h2}e_{h3} + O_{h2} - \bar{k}_{\gamma 3}e_{h3}^2 + \frac{\ell_{\gamma 2}\eta_h^{*2}}{4} + \frac{1+\varpi_{2\max}^2}{4\ell_{\gamma 1}} - e_{h2}e_{h3} + O_{h3} \\
&= -\bar{k}_{\gamma 1}e_{h1}^2 - \bar{k}_{\gamma 2}e_{h2}^2 - \bar{k}_{\gamma 3}e_{h3}^2 + \frac{\ell_{\gamma 2}\eta_h^{*2}}{4} + \frac{1+\varpi_{2\max}^2}{4\ell_{\gamma 1}} + O_h \\
&\le -\mathfrak{g}J_h + C
\end{aligned} \tag{77}$$

where $\mathfrak{g} = \min\{\bar{k}_{\gamma 1}, \bar{k}_{\gamma 2}, \bar{k}_{\gamma 3}\}$, $C = \ell_{\gamma 2}\eta_h^{*2}/4 + (1+\varpi_{2\max}^2)/(4\ell_{\gamma 1}) + O_h$, $O_h \triangleq O_{h1} + O_{h2} + O_{h3}$. Then the closed-loop system (5) is semi-globally stable and all the signals involved are bounded. Wherein, the tracking error between $\gamma$ and $\gamma_d$ is invariant to the following set

$$\Omega_{e_{h1}} = \left\{ e_{h1} \middle| |e_{h1}| \le \sqrt{C/\mathfrak{g}} \right\} \tag{78}$$

The radius of $\Omega_{e_{h1}}$ can be made arbitrarily small by choosing sufficiently large $\bar{k}_{\gamma 1}$, or $\bar{k}_{\gamma 2}$ or $\bar{k}_{\gamma 3}$. When $\gamma \to \gamma_d$, then $h \to h_r$ as seen from equation (1). And the transient and steady-performance defined in equation (51) can be preserved. This completes the proof of Theorem 4.

**Remark 4.** Compared with previous works,[10–13] only two parameters need to be reduced online in the

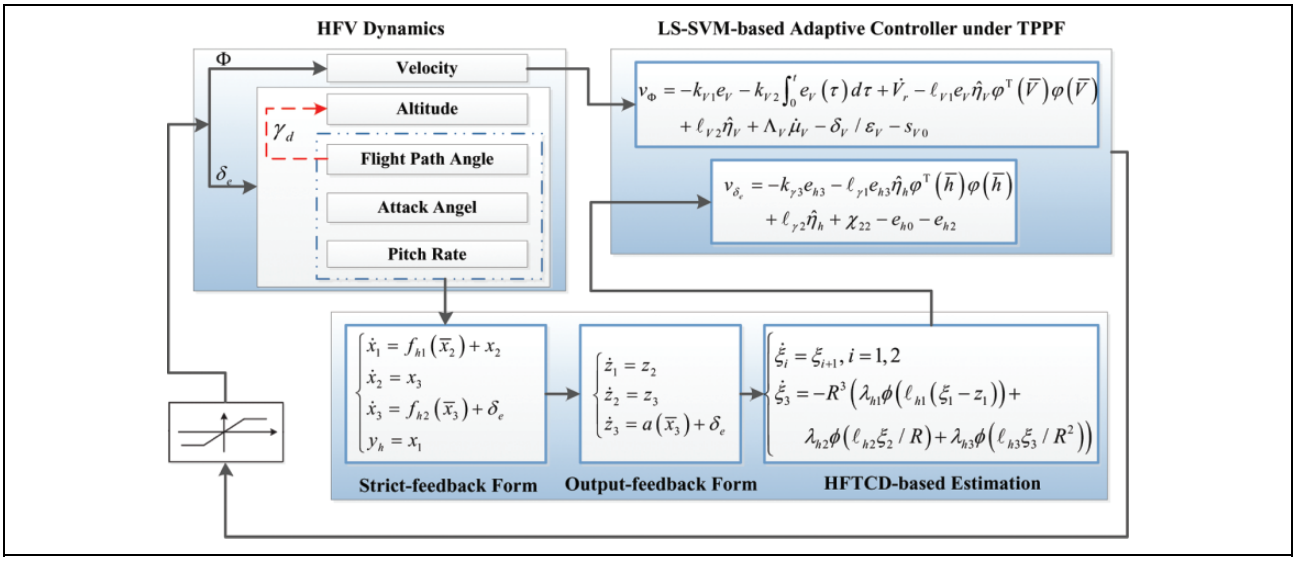


**Figure 3.** The control scheme constructed in this work.

nonlinearity approximation. Meanwhile, only two design parameters are required in two LS-SVM-based approximators and the relevant solutions to the weights are addressed by solving two linear functions without specific optimization algorithms. This drops the complexity of computation dramatically. Thus, the LS-SVM-based approximation is advantageous for the online approximation of unknown hypersonic dynamics.

**Remark 5.** The newly developed HFTCD are applied to obtain the estimation for the newly defined state variables and the derivatives of the devised virtual controllers with small estimation errors within finite time. Whilst, the tedious analysis and repeated derivations of the virtual controllers are avoided. Thus, the inherent limitation of the backstepping technique — "explosion of terms" is conquered.

Figure 3 shows the control scheme constructed in this work, which will be validated in the following numerical simulations.

## Numerical simulations

The proposed controllers in equations (45) and (71) with the adaptation schemes in equations (46) and (72) are tested for the system given by equation (1). Wherein, the newly developed HFTCD is tested by estimating the unknown state variables, and the derivatives of virtual controllers. The aerodynamic coefficients and model parameters refer to the work by Xu et al.[11] The reference commands are generated by the following filter

$$\frac{V_r}{V_c} = \frac{0.5 \times 0.3^2}{(s+0.5)(s^2 + 2 \times 0.7 \times 0.3s + 0.3^2)} \tag{79a}$$

$$\frac{h_r}{h_c} = \frac{0.5 \times 0.2^2}{(s+0.5)(s^2 + 2 \times 0.7 \times 0.2s + 0.2^2)} \tag{79b}$$

The detailed chosen parameters involved in the control system are provided in Table 1. Wherein, the design parameters of both two LS-SVM-based approximators are set as the same.

The initial values involved in the simulations are set, respectively, as $V_0 = 7850$ ft/s, $h_0 = 86000$ ft, $\gamma_0 = 0$, $q_0 = 0$, and $\alpha = 3.5^\circ$. The velocity tracks the given step command with 200 ft/s every 60 s. Whilst, the altitude tracks the square command with a period of 120 s and and amplitude of 1000 ft. The actuator saturations of $\Phi$ and $\delta_e$ considered in the simulation are depicted in Figures 1 and 2, respectively.

The simulation results are portrayed from Figures 4 to 15. In detail, one can conclude the following.

1. Seeing from Figures 4 to 8, under the LS-SVM-based adaptive controllers subject to actuator saturation, the velocity and altitude commands are rapidly tracked, respectively. And the steady-state tracking errors lie in a small domain near the origin which satisfy the limitations induced by the TPPF.
2. As portrayed in Figures 9 to 11, the devised LS-SVM-based approximator and HFTCD obtain good approximations for unknown nonlinear functions, state variables, and the derivatives of the virtual controllers with high accuracy, respectively. Consequently, the inherent demerit of the backstepping technique – "explosion of terms" is overcome.
3. In order to test the superiority of the proposed TPPF compared with the CPPF, the relevant simulation results are shown in Figures 14 and 15 under the same initial simulation conditions. Wherein, one can find that steady-state tracking errors attain up to a $10^{-2}$ order of magnitude under the TPPF. While, the steady-state tracking errors under CPPF are at the level of $10^{-1}$. Hence, the proposed TPPF

**Table 1.** The values of the design parameters.

| Equations | Values |
|---|---|
| LS-SVM in equation (16) | $c_0 = 1000$, $\zeta^2 = 0.3$ |
| TPPF in equations (40) and (51) | $\kappa_{V1} = 0.01$, $\kappa_{V2} = 0.01$, $\delta_{V10} = 5$, $\delta_{V20} = 2.5$, $\delta_{V1\infty} = 0.2$, $\delta_{V2\infty} = 0.2$<br>$\kappa_{h1} = 0.015$, $\kappa_{h2} = 0.01$, $\delta_{h10} = 2$, $\delta_{h20} = 1$, $\delta_{h1\infty} = 0.2$, $\delta_{h2\infty} = 0.2$<br>$\mu_V = \mu_h = \mu$, $\kappa_\mu = 0.05$, $\mu_0 = 3$, $\mu_\infty = 0.1$ |
| Equations (45) and (46) | $k_{V1} = 2$, $k_{V2} = 0.5$, $\ell_{V1} = 0.02$, $\ell_{V2} = 0.001$, $\Gamma_V = 1$ |
| Equations (57), (71) and (72) | $k_{h1} = 2$, $k_{h2} = 0.5$, $k_{\gamma 1} = 2$, $k_{\gamma 2} = 1.5$, $k_{\gamma 3} = 1$<br>$\Gamma_h = 1$, $\ell_{\gamma 1} = 0.01$, $\ell_{\gamma 2} = 0.001$ |
| HFTCD in equations (55), (63) and (69) | $R = 2.5$, $\lambda_{h1} = \lambda_{h2} = \lambda_{h3} = 2$, $\ell_{h1} = 1$, $\ell_{h2} = \ell_{h3} = 3$<br>$R_{11} = 3$, $\lambda_{11} = 5$, $\lambda_{12} = 3$, $\ell_{11} = \ell_{12} = 2$<br>$R_{22} = 5$, $\lambda_{21} = 1$, $\lambda_{22} = 2$, $\ell_{21} = \ell_{22} = 1$ |

LS-SVM: least square support vector machine; TPPF: time-varying predefined performance function; HFTCD: hyperbolic finite-time-convergent differentiator.

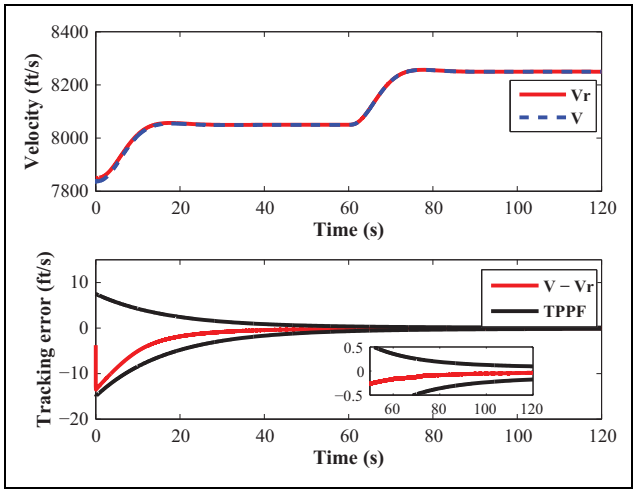


**Figure 4.** Velocity tracking trajectory.

is advantageous in obtaining high tracking accuracy compared with the CPPF.

Based on the illustrative results, from another perspective, one can further obtain that the proposed TPPF can be seen as an additive time-varying semi-enclosed constraint given by the designers. The time-varying semi-enclosed constraint forms a tube where the transient and steady-state performance of controlled systems is permitted. If the tube changes fast (i.e. large positive real numbers for the parameters $\kappa_0$, $\kappa_1$, and $\kappa_2$ in equation (7) are chosen) with a small upper and lower bound (i.e. small positive real numbers for the parameters $\delta_{1\infty}$, $\delta_{2\infty}$, and $\mu_\infty$ in equation (7) are chosen), a fast dynamic response and high tracking accuracy can be

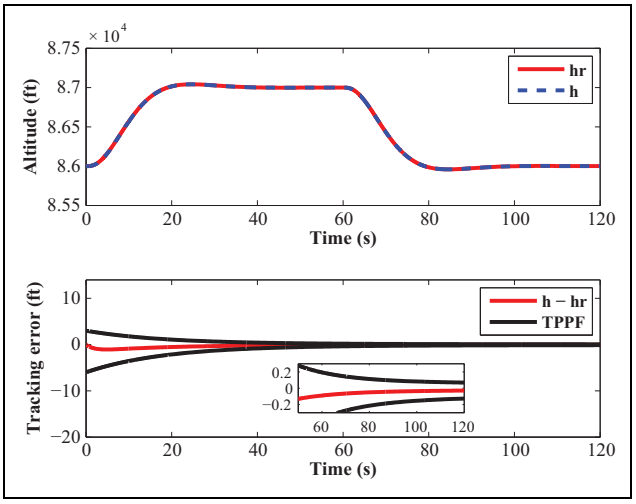


**Figure 5.** The altitude tracking trajectory.

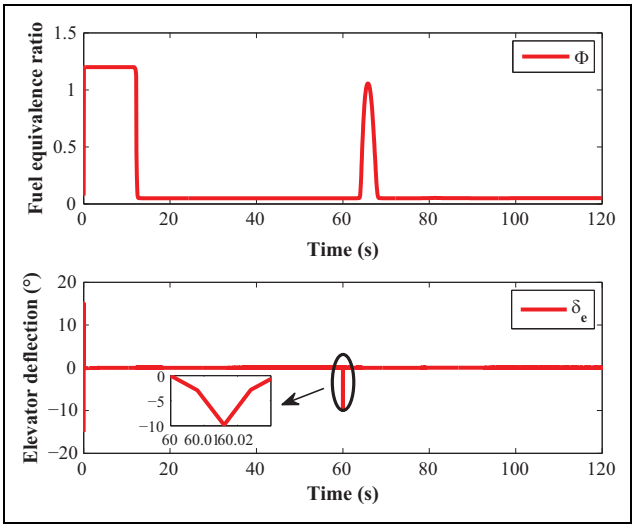


**Figure 6.** Fuel equivalence ratio and elevator deflection.

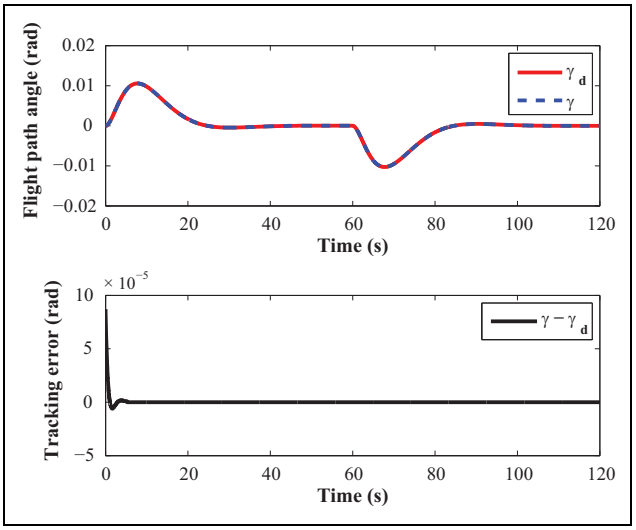


**Figure 7.** The flight angle.

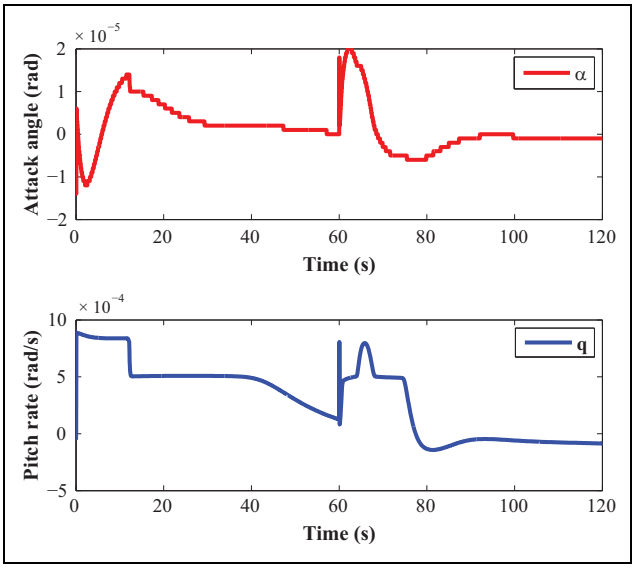


**Figure 8.** Attack angle and pitch rate.

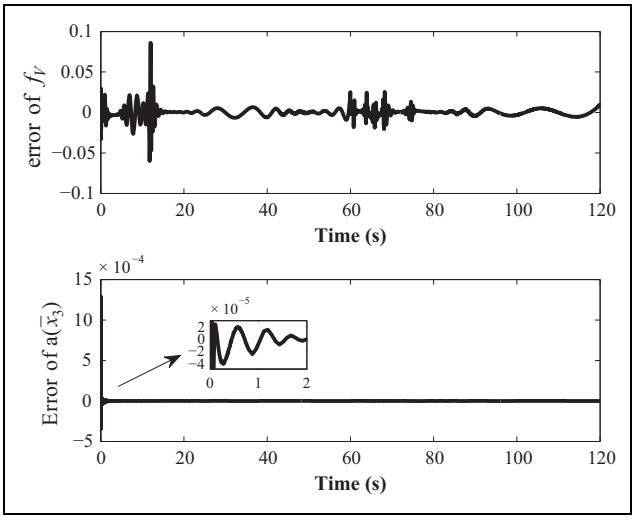


**Figure 9.** LS-SVM-based approximation errors of $f_V$ and $a(\bar{x}_3)$.

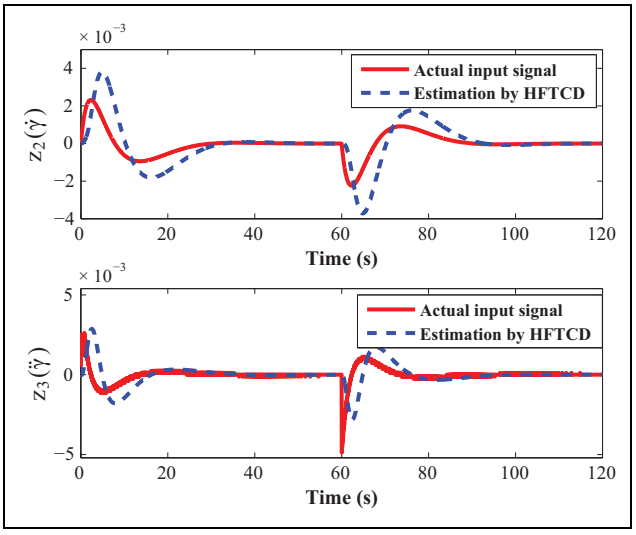


**Figure 10.** HFTCD-based estimations of $z_2$ and $z_3$.

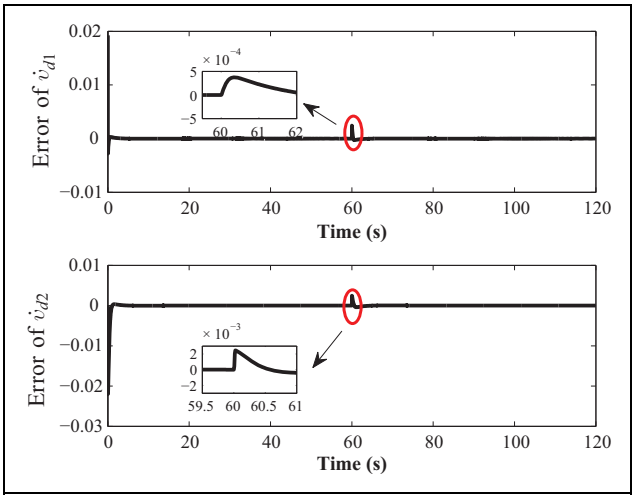


**Figure 11.** HFTCD-based approximation errors of $\dot{v}_{d1}$ and $\dot{v}_{d2}$.

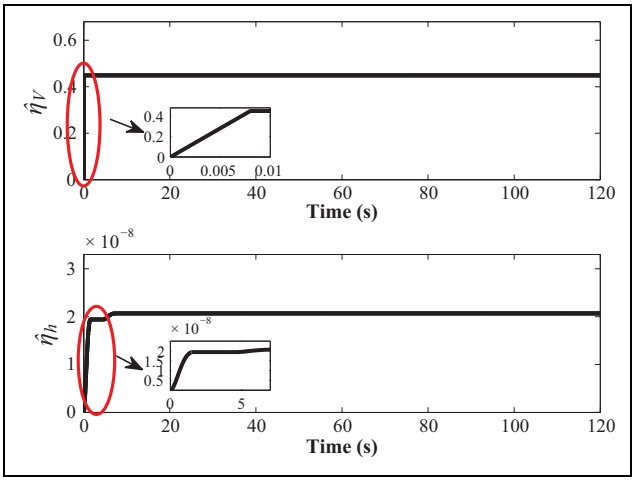


**Figure 12.** Estimations of $\eta_V$ and $\eta_h$.

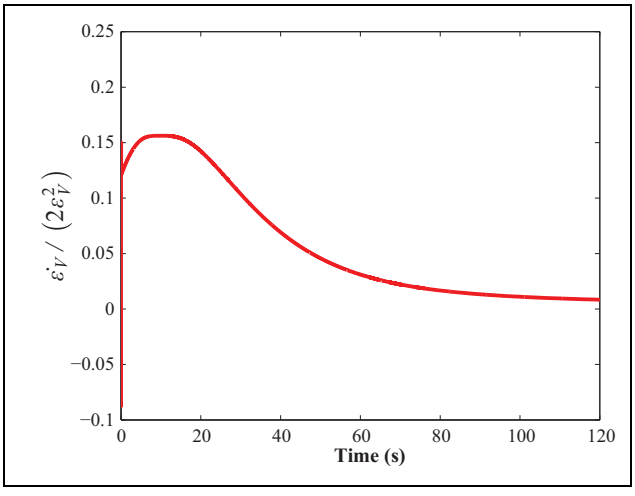


**Figure 13.** Curve of $\dot{\varepsilon}_V/(2\varepsilon_V^2)$ in the inequality given by equation (52).

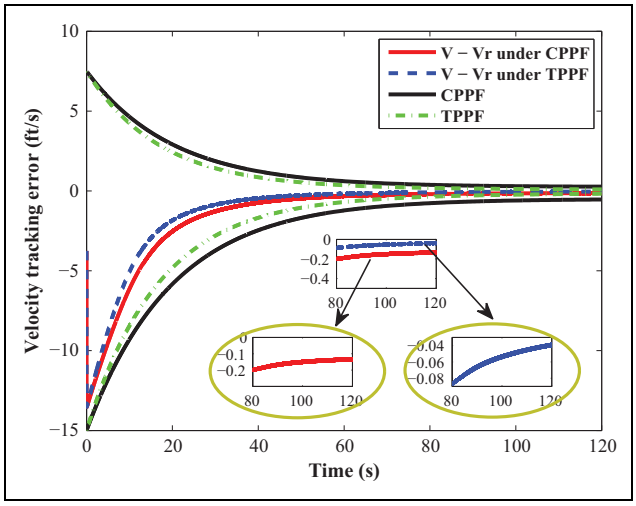


**Figure 14.** Velocity tracking errors under the TPPF and the CPPF.

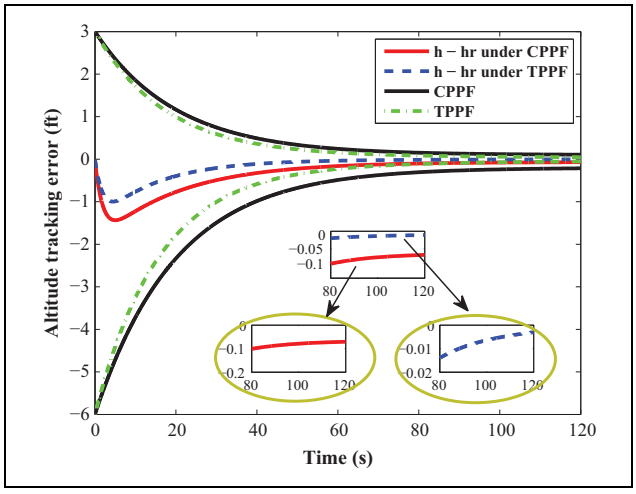


**Figure 15.** Altitude tracking errors under the TPPF and the CPPF.

obtained. However, large control efforts are needed and the saturation of actuator easily occurs, just like the depiction in Figure 6. Thus, a trade-off between the tracking accuracy and fuel consumption as well as the system reliability should be considered from the perspective of engineering.

## Conclusions

A computationally fast adaptive control method under a TPPF in the presence of unknown nonlinearities and actuator saturation, is proposed for HFV in this article. Based on functional decomposition, two LS-SVM-based adaptive controllers are, respectively, devised to track the velocity and altitude commands. Wherein, by applying the newly developed HFTCD to estimate the newly defined state variables, the complex strict-feedback formulation is completely avoided. Meanwhile, the derivatives of virtual controllers are estimated by the newly developed HFTCD with errors at the level of $10^{-3}$. So no tedious analysis and computation of the derivations of the virtual controllers are needed. Thereby, the inherent drawback of the backstepping technique – "explosion of terms" is conquered. Besides, only two LS-SVM-based approximators with two adaptive scalars are required to approximate the unknown hypersonic dynamics. Compared with the NN, only two design parameters in the LS-SVM are needed and the ideal weight is obtained through solving a linear system rather than tedious optimizations. Consequently, the computational burden is significantly reduced. Thus, the LS-SVM technique is very advantageous in the approximation of unknown nonlinearities of the HFV online.

The simulation results demonstrate that the proposed controllers can preserve the transient performance defined by the TPPF. Moreover, the proposed controllers can track the velocity and altitude commands with steady-state errors at the level of $10^{-2}$, which are about 1 order of magnitude smaller than those under the CPPF. Thus, the proposed TPPF is superior to the CPPF in terms of the steady-state errors.

## Declaration of conflicting interests

The author(s) declared no potential conflicts of interest with respect to the research, authorship, and/or publication of this article.

## Funding

The author(s) disclosed receipt of the following financial support for the research, authorship, and/or publication of this article: This work was supported in part of the Major Program of National Natural Science Foundation of China under Grants 61690210 and 61690211, the National Natural Science Foundation of China under Grants 11502203 and 61603304, and the Innovation Foundation for Doctor Dissertation of Northwestern Polytechnical University under Grant CX201602.

## References

1. Xu B and Shi Z. An overview on flight dynamics and control approaches for hypersonic vehicles. *Sci China Inform Sci* 2015; 58(7): 1–19.
2. Xu H, Mirmirani MD and Ioannou PA. Adaptive sliding mode control design for a hypersonic flight vehicle. *J Guid Control Dyn*; 27(5): 829–838.
3. Fiorentini L, Serrani A, Bolender MA, et al. Nonlinear robust adaptive control of flexible air-breathing hypersonic vehicles. *J Guid Control Dyn* 2009; 32(2): 402–417.
4. Shen Q, Jiang B and Cocquempot V. Fault-tolerant control for T-S fuzzy systems with application to near-space hypersonic vehicle with actuator faults. *IEEE T Fuzzy Syst* 2012; 20(4): 652–665.
5. Hu X, Wu L, Hu C, et al. Fuzzy guaranteed cost tracking control for a flexible air-breathing hypersonic vehicle. *IET Control Theory A* 2012; 6(9): 1238–1249.
6. Xu B, Wang S, Gao D, et al. Command filter based robust nonlinear control of hypersonic aircraft with magnitude constraints on states and actuators. *J Intell Robot Syst* 2014; 73(1): 233–247.
7. Cai G, Duan G, Hu C, et al. Tracking control for air-breathing hypersonic cruise vehicle based on tangent linearization approach. *J Syst Eng Electron* 2010; 21(3): 469–475.
8. Wu G and Meng X. Nonlinear disturbance observer based robust backstepping control for a flexible air-breathing

hypersonic vehicle. *Aerosp Sci Technol* 2016; 54: 174–182.
9. Xu B, Yang C and Pan Y. Global neural dynamic surface tracking control of strict-feedback systems with application to hypersonic flight vehicle. *IEEE Trans Neural Netw Learn Syst* 2015; 26(10): 2563–2575.
10. Xu B. Robust adaptive neural control of flexible hypersonic flight vehicle with dead-zone input nonlinearity. *Nonlinear Dyn* 2015; 80(3): 1509–1520.
11. Xu B, Huang X, Wang D, et al. Dynamic surface control of constrained hypersonic flight models with parameter estimation and actuator compensation. *Asian J Control* 2014; 16(1): 162–174.
12. Chen M, Tao G and Jiang B. Dynamic surface control using neural networks for a class of uncertain nonlinear systems with input saturation. *IEEE Trans Neural Netw Learn Syst* 2015; 26(9): 2086–2097.
13. Xu B, Zhang Q and Pan Y. Neural network based dynamic surface control of hypersonic flight dynamics using small-gain theorem. *Neurocomputing* 2016; 173(P3): 690–699.
14. Butt WA, Yan L and Amezquita SK. Adaptive integral dynamic surface control of a hypersonic flight vehicle. *Int J Syst Sci* 2015; 46(10): 1717–1728.
15. Bu X, Wu X, Zhang R, et al. Tracking differentiator design for the robust backstepping control of a flexible air-breathing hypersonic vehicle. *J Franklin Inst* 2015; 352(4): 1739–1765.
16. Gao D, Wang S and Zhang H. A singularly perturbed system approach to adaptive neural back-stepping control design of hypersonic vehicles. *J Intell Robot Syst* 2014; 73(1-4): 249–259.
17. Vapnik V. *Statistical learning theory*. New York: Springer, 1998.
18. Suykens JAK and Vandewalle J. Least squares support vector machine classifiers. *Neural Process Lett* 1999; 9(3): 293–300.
19. Wang Z, Zhang Z and Mao J. Adaptive tracking control based on online LS-SVM identifier. *Int J Fuzzy Syst* 2012; 14(2): 330–336.
20. Li Z, Zhang Y and Yang Y. Support vector machine optimal control for mobile wheeled inverted pendulums with unmodelled dynamics. *Neurocomputing* 2010; 73(13): 2773–2782.
21. Gu Y, Zhao W and Wu Z. Online adaptive least squares support vector machine and its application in utility boiler combustion optimization systems. *J Process Control* 2011; 21(7): 1040–1048.
22. Bechlioulis CP and Rovithakis GA. Robust adaptive control of feedback linearizable MIMO nonlinear systems with prescribed performance. *IEEE Trans Automat Contr* 2008; 53(9): 2090–2099.
23. Bechlioulis CP and Rovithakis GA. Adaptive control with guaranteed transient and steady state tracking error bounds for strict feedback systems. *Automatica* 2009; 45(2): 532–538.
24. Na J. Adaptive prescribed performance control of nonlinear systems with unknown dead zone. *Int J Adapt Control Signal Process* 2013; 27(5): 426–446.
25. Yoo SJ. Distributed containment control with predefined performance of high-order multi-agent systems with unknown heterogeneous non-linearities. *IET Control Theory A* 2015; 9(10): 1571–1578.
26. Chen M, Liu X and Wang H. Adaptive robust fault-tolerant control for nonlinear systems with prescribed performance. *Nonlinear Dyn* 2015; 81(4): 1727–1739.
27. Yang Q and Chen M. Adaptive neural prescribed performance tracking control for near space vehicles with input nonlinearity. *Neurocomputing* 2016; 174: 780–789.
28. Bu X, Wu X, Huang J, et al. A guaranteed transient performance-based adaptive neural control scheme with low-complexity computation for flexible air-breathing hypersonic vehicles. *Nonlinear Dyn* 2016; 84(4): 2175–2194.
29. Parker JT, Serrani A, Yurkovich S, et al. Control-oriented modeling of an air-breathing hypersonic vehicle. *J Guid Control Dyn* 2007; 30(3): 856–869.
30. Xu B, Fan Y and Zhang S. Minimal-learning-parameter technique based adaptive neural control of hypersonic flight dynamics without back-stepping. *Neurocomputing* 2015; 164: 201–209.
31. Haimo VT. Finite time controllers. *SIAM J Control Optim* 1986; 24(4): 760–770.
32. Bhat SP and Bernstein DS. Finite-time stability of continuous autonomous systems. *SIAM J Control Optim* 2000; 38(3): 751–766.
33. Wang X, Chen Z and Yang G. Finite-time-convergent differentiator based on singular perturbation technique. *IEEE Trans Automat Contr* 2007; 52(9): 1731–1737.
34. Wang X and Lin H. Design and frequency analysis of continuous finite-time-convergent differentiator. *Aerosp Sci Technol* 2012; 18(1): 69–78.

# Appendix

## Notation

| | | |
|---|---|---|
| $C_D^{\alpha^i}$ | = | $i$ th order coefficient of $\alpha$ in $D$ |
| $C_L^{\alpha^i}$ | = | $i$ th order coefficient of $\alpha$ in $L$ |
| $C_M^{\alpha^i}$ | = | $i$ th coefficient of $\alpha$ in $M$ |
| $C_M^{\delta_e}$ | = | coefficient of $\delta_e$ in $M$ |
| $h$, $h_r$ | = | altitude and reference altitude |
| $h_0$, $1/h_s$ | = | nominal attitude for air density approximation and air density decay rate |
| $I_{yy}$, $M_{yy}$ | = | moment of inertial axis and pitch moment |
| $m$, $g$ | = | vehicle mass and gravitational acceleration |
| $\mathbb{R}$, $I$ | = | set of real numbers and identity matrix of approximate dimensions |
| $\mathbb{R}^n$ | = | $n$-dimensional Euclidean space |
| $S_a$, $\bar{c}$, $z_T$ | = | reference area, mean aerodynamic chord and thrust moment arm |
| $T$, $L$, $D$ | = | thrust, lift and drag |
| $V$, $V_r$ | = | velocity and reference velocity |
| $\beta_i (i = 1, 2, \ldots, 8)$ | = | thrust fit coefficient |
| $\delta_e$, $\Phi$ | = | elevator deflection and fuel equivalence ratio |
| $\gamma$, $\alpha$, $q$ | = | flight path angle, attack angle, pitch rate |
| $\bar{q}$, $\gamma_d$ | = | dynamic pressure and reference flight path angle |
| $\rho$, $\rho_0$ | = | density of air and nominal air density at the altitude $h_0$ |
| $\lvert \bullet \rvert$ | = | the absolute value of a scalar |
| $\lVert \bullet \rVert$ | = | 2-norm of a vector |